Atomic Energy Control Board
P.O. Box 1046
Ottawa, Canada
K1P 5S9

Commission de contrôle de l'énergie atomique
C.P. 1046
Ottawa, Canada
K1P 5S9

INFO-0391

THE PROLIFERATIVE CELLS OF THE HUMAN BRONCHIAL EPITHELIUM

(AECB Project No. 4.121.2)

by

F. Baldwin
Department of Pathology
Faculty of Medicine
University of Manitoba

A research report prepared for the
Atomic Energy Control Board
Ottawa, Canada

Published November 1991

Canada

Research report

92-05916/

PROLIFERATING CELLS IN HUMAN BRONCHIAL EPITHELIUM

A report by Frank Baldwin, Ph.D. under contract to the Atomic Energy Control Board.

ABSTRACT

Basal Cells have long been regarded as progenitors of human bronchial epithelium and important in the development of lung cancer but most data pertaining to laboratory animals indicate the basal cell may not be the sole proliferative element.

The objectives of the present study were 1) to identify and enumerate the proliferating cells of the airways, 2) to establish the nature of typical and atypical basal cells, 3) to determine the ultrastructure of basal cells and their relationship to adjacent cells, and 4) to relate the information obtained to physiological parameters of importance to radiation dosimetry.

Assessment of cell proliferation was tested in tissue known to contain substantial populations of proliferating cells, following which proliferating cells were identified in multiple bronchi from seven adult surgical cases by Ki-67 immunolabelling. In 8 μm cross sections of bronchi (Generations 7-15) labelled typical basal cells comprised the majority (1 cell/mm epithelium). There were fewer labelled atypical basal cells (1 cell/3mm epithelium) and labelled unciliated columnar cells (1 cell/5mm epithelium), but no significant differences between generations. The percentage of typical basal cell proliferating ranged from 0.8% - 2.8%; for atypical basal cells the proliferating population ranged from 0.4% - 2.1%. Many focal areas of metaplasia were unlabelled. However some areas contained large numbers of labelled cells, reflecting intense proliferative activity. There were more proliferating basal cells in bronchi from former smokers than from smokers. Since all cells are within range of α particles, emitted from radioactive sources deposited at the mucociliary surface, typical basal cells, atypical basal cells and columnar cells are all at risk.

Columnar cells are joined to one another at junctions. The basal aspect of columnar cells extends into processes, rather like the root of a tooth. Where the cytoplasm contacts the basement membrane there are no recognizable means of attachment, but there are junctions where columnar cells contact underlying atypical basal cells. Columnar cells are also attached to the lateral aspects of typical pyramidal basal cells. Whilst atypical basal cells individually represent a larger surface for attachment than typical basal cells, the latter because of their superior numbers, are important in epithelial cohesion. Neither type of basal cells possesses contractile filaments.

RÉSUMÉ

On soutient depuis longtemps que, chez l'homme, les cellules de l'épithélium bronchique naissent des cellules basales qui jouent un rôle important dans le développement du cancer. Par contre, la plupart des données provenant des études faites sur des animaux de laboratoire indiquent que la cellule basale n'est peut-être pas la seule qui prolifère.

La présente étude visait à : (1) déterminer et dénombrer les cellules proliférantes dans les voies respiratoires; (2) déterminer la nature des cellules basales typiques et atypiques; (3) déterminer l'ultrastructure des cellules basales, ainsi que leur rapport avec les cellules adjacentes, et (4) établir un rapport entre les données ainsi obtenues et les paramètres physiologiques importants en dosimétrie des rayonnements.

La prolifération des cellules a d'abord été examinée dans des échantillons de tissu contenant des nombres importants de cellules proliférantes qui ont été identifiées (immuno-identification Ki-67) dans plusieurs échantillons de bronches prélevés sur sept adultes par voie chirurgicale. Dans les coupes transversales de 8 µm de bronches des générations 7 à 15, les cellules basales typiques identifiées composaient la majorité (1 cellule par millimètre d'épithélium). Il y avait un nombre moins élevé de cellules basales atypiques identifiées (1 cellule par 3 mm d'épithélium), et de cellules non ciliées en forme de colonne (1 cellule par 5 mm d'épithélium), mais il n'y avait aucune différence importante entre les diverses générations. Le pourcentage des cellules basales typiques en voie de prolifération était de 0,8 % à 2,8 % et celui des cellules basales atypiques était de 0,4 % à 2,1 %. De nombreux foyers de métaplasie n'ont pas été marqués. Cependant, certaines zones contenaient de nombreuses cellules marquées, indiquant une activité proliférative intense. Les cellules basales proliférantes étaient plus nombreuses dans les échantillons de bronches des fumeurs que dans ceux des non-fumeurs. Étant donné que toutes les cellules se trouvent à la portée des particules alpha émises par des sources radioactives situées à la surface mucociliaire, les cellules basales typiques, les cellules basales atypiques et les cellules en forme de colonne sont toutes exposées au risque des rayonnements.

Les cellules en forme de colonne sont attachées l'une à l'autre aux jonctions. L'aspect basal des cellules en forme de colonne s'étend vers le bas de la même façon que la racine des dents. Là où le cytoplasme touche la membrane sous-jacente, il n'existe aucun moyen de fixation observable, mais il y a des jonctions où des cellules en forme de colonne touchent les cellules basales atypiques sous-jacentes. Des cellules en forme de colonne se rattachent également aux éléments latéraux des cellules basales typiques pyramidales. Alors que les cellules basales atypiques présentent chacune une plus grande surface propice au rattachement que les cellules basales typiques, celles-ci, en raison de leur plus grand nombre, jouent un rôle important dans la cohésion de l'épithélium. Ni les

cellules basales typiques ni les cellules basales atypiques ne contiennent de filament contractile.

DISCLAIMER

The Atomic Energy Control Board is not responsible for the accuracy of the statements made or opinions expressed in this publication and neither the Board nor the authors assume liability with respect to any damage or loss incurred as a result of the use made of the information contained in this publication.

TABLE OF CONTENTS

	Page
ABSTRACT	i
DISCLAIMER	iii
LIST OF FIGURES	vii
LIST OF TABLES	ix
A. INTRODUCTION	1
1. Background	1
2. Microscopic Anatomy of Bronchial Epithelium	2
3. Assessment of Cell Proliferation	2
4. Objectives of the Study	5
B. MATERIALS AND METHODS	5
1. Proliferating Cells in Control Tissue	5
1.1. Materials	5
1.2. Methods	5
1.2.1. Freezing technique	5
1.2.2. Sections	6
1.2.3. Fixation	6
1.2.4. Immunostaining	6
2. Proliferating Cells in Adult Epithelium	8
2.1. Materials	8
2.2. Methods	9
2.2.1. Freezing technique	9
2.2.2. Fixation and processing for light microscopy	9
2.2.3. Fixation and processing for electron microscopy	9
2.2.4. Ki-67 immunostaining	9
2.2.5. BrdU immunostaining	10
2.3. Morphometry	10
2.3.1. Selection of bronchi	10
2.3.2. Measurement of bronchi	10
2.3.3. MOP videoplan image analysis system	10
2.3.4. Cell enumeration	11
2.4 Statistical Methods	11
C. RESULTS	11
1. Detection of Proliferating Cells in Control Tissue	11
2. Detection of Proliferating Cells in Adult Lung	12
3. Basal Cell Morphology	14
4. Basal Cell Morphometry	16
D. DISCUSSION	17

REFERENCES

ACKNOWLEDGEMENTS

APPENDIX A: Surface to Nuclear Distances in Human Bronchial Epithelium: Relations to Penetration by Rn Daughters

LIST OF FIGURES

		Page
FIGURE 1	Bronchial epithelium	2a
FIGURE 2	Average diameter of airways in human lung	2a
FIGURE 3	The cell cycle	2b
FIGURE 4	Foetal lung Haematoxylin stain	2b
FIGURE 5	Foetal lung Ki-67 technique	7a
FIGURE 6	Tumor Brd U technique	7a
FIGURE 7	Bronchial epithelium Ki-67 technique	9a
FIGURE 8	Bronchial lymphoid tissue from same preparation as Figure 7	9a
FIGURE 9	Bronchial epithelium Ki-67 technique	12a
FIGURE 10	Metaplastic bronchial epithelium Ki-67 technique	12a
FIGURE 11	Bronchial epithelium	14a
FIGURE 12	Typical basal cell	14a
FIGURE 13	Atypical basal cell and columnar cell	14a
FIGURE 14	Atypical basal cell and columnar cells	15a
FIGURE 15	Atypical basal cell	15a
FIGURE 16	Atypical basal cell and columnar cells	15b
FIGURE 17	Atypical basal cell cytoplasm	15b
FIGURE 18	Atypical basal cell cytoplasm	15b
FIGURE 19	Atypical basal cell	15c
FIGURE 20	Contacts between atypical basal cells	15c
FIGURE 21	Contacts between atypical basal cells	15c
FIGURE 22	Contacts between basal cells	15d
FIGURE 23	Basal cells present as two layers of cells	15d
FIGURE 24	Bronchial gland	15e
FIGURE 25	Bronchial epithelium	15e

FIGURE 26 Myoepithelial cell 15f

FIGURE 27 Myoepithelial cell cytoplasm 15f

FIGURE 28 Epithelial and basal cell measurements 16a

FIGURE 29 Distances: lumenal surface to basal cell nucleus, adjacent epithelium 16a

LIST OF TABLES

		Page
TABLE 1	Ki-67 Labelled Basal and Columnar Cells and Total Basal Cells	22
TABLE 2	Ki-67 Labelled Basal and Columnar Cells and Total Basal Cells per mm of Epithelium	23
TABLE 3A	Analysis of Labelled Cells per mm of Epithelium	25
TABLE 3B	Analysis of Basal Cells per mm of Epithelium	25
TABLE 4A	Labelled Basal Cells as a Percentage of Total Basal Cells	27
TABLE 4B	Analysis of Labelled Basal Cells as a Percentage of Total Basal Cells	28
TABLE 5A	Ki-67 Labelled Cells per mm Length of Bronchi by Generations	29
TABLE 5B	Ki-67 Labelled Cells in Each Bronchial Generation	29
TABLE 6A	Comparisons Between Smokers and Ex-smokers Ki-67 Labelled Cells per mm Epithelium	30
TABLE 6B	Comparisons Between Smokers and Ex-smokers Basal Cells per mm Epithelium	31
TABLE 6C	Comparisons Between Smokers and Ex-smokers Ki-67 Labelled Basal Cells as a Percentage of Total Basal Cells per mm Epithelium	32
TABLE 7	Epithelial Measurements (μm)	33

A. INTRODUCTION

1. Background

The cytokinetics of human bronchial epithelium are poorly understood. For many years basal cells have been regarded as progenitors of human bronchial epithelium (Spencer, 1985; Ayers and Jeffery, 1982) and it has been held widely that proliferation of basal cells is of paramount importance in the development of lung cancer (Auerbach, 1980).

Animal studies show the basal cell to be an epithelial progenitor (Ayers and Jeffery, 1982; Bindreiter et al, 1968; Boren and Paradise, 1978; Donnelly, et al, 1982; Evans et al, 1986; Inayama et al 1988, 1989; Lane and Gordon, 1974), but although basal cells show greater proliferative activity and act as stem cells, secretory cells also contribute to cell renewal (Bindreiter et al, 1968; Boren and Paradise, 1978; Breuer et al, 1990) and replicate in response to acute injury (Evans et al, 1986; Keenan et al, 1982a and b).

Thus from animal studies there are indications that the basal cell may not be the only proliferative cell in bronchi and is not necessarily the dominant cell in epithelial replacement. Proliferation has been detected in several cell types in bronchial epithelium of various animals (Ayers and Jeffery, 1988); basal, serous, mucous and non-ciliated secretory cells have the capacity to divide, the number and proportion of each contributing to the dividing cell population varies with airway level. Several animal investigations (Bindreiter et al, 1968; Lane and Gordon, 1974; Becci et al, 1978; Boren and Paradise, 1978; Donnelly et al, 1982; Evans et al, 1986) show that both basal and non-ciliated columnar cells with or without secretory granules, are capable of DNA synthesis and/or cell division; while ciliated cells are non-proliferative.

In contrast to the larger airways, there are no basal cells in the terminal and respiratory bronchioles. At these sites, the Clara cell is considered to be the proliferative unit. In the alveolar epithelium, the type II cell is the sole progenitor.

Many of the studies of epithelial kinetics have been limited to the trachea. Boren and Paradise (1978) identified two kinetic compartments: self maintaining tracheal basal cells which yield a dividing mucous cell population, the precursors of functioning mucous, and ciliated cells.

In other studies of the trachea, basal cells replicated to produce only basal cells in the hamster (McDowell et al, 1985) and monkey (Plopper et al, 1986). Notwithstanding the regenerative capacity of secretory cells, it seems that basal cells are the real stem cells because they can give rise to all types of epithelium (Inayama et al, 1988).

Most of these data pertain to laboratory animals. Little is known about proliferative cells in human bronchial epithelium because the in vivo labelling techniques used for kinetic studies in experimental animals (Bertanlanffy and Leblond, 1953) are not readily transferable to human studies. The availability of markers to detect antigens present in human proliferating cells in histological sections provides a new tool for this type of investigation.

2. Microscopic anatomy of bronchial epithelium

Much of what is known about the morphology of the bronchial epithelium has been derived from studies of young animals free of respiratory disease or the modifying effects of irritants. At least eight cell types are recognized (Ayers and Jeffrey, 1988); fewer epithelial cells have been recognized with certainty in human bronchial epithelium.

The human bronchus is lined by a pseudostratified epithelium, the components of which are illustrated in Figure 1. The basal cell population is comprised of two elements, a typical pyramidal basal cell and an elongated atypical cell. Whilst the proliferative role for basal cells has long been proposed, they may serve an additional function: anchoring of columnar cells to the basement membrane (Evans and Plopper, 1988; Evans et al, 1989). Basal cells usually are separated from one another by the cytoplasm of columnar cells. They may also form a continuous layer and occasionally there may be more than one layer of basal cells (McDowell and Beals, 1986).

Dense core granule cells, also known as neurendocrine cells or Kultchitsky cells, occur principally in clusters at bronchial bifurcations, but are found less frequently elsewhere in the epithelium of adults.

With progressive divisions of the human bronchial tree, bronchial size diminishes (Weibel, 1963) (Figure 2), the epithelium decreases in thickness and the proportions of cells varies with the level of the airway (Bowden and Baldwin, 1989; Baldwin et al, 1991).

3. Assessment of cell proliferation

The cell cycle is divided into several distinct phases, with considerable variation in their duration in different cell types. DNA is replicated during a short period (S Phase) (Figure 3). The M phase (mitosis or cell division) is of short duration also and, in tissues with a low rate of turnover, the chance of finding a mitotic figure is small.

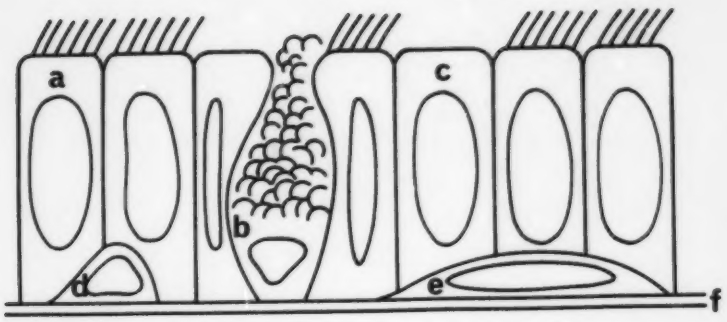

Figure 1 Bronchial epithelium
a) ciliated columnar cell
b) goblet cell
c) unciliated columnar cell
d) typical basal cell
e) atypical basal cell
f) basement membrane

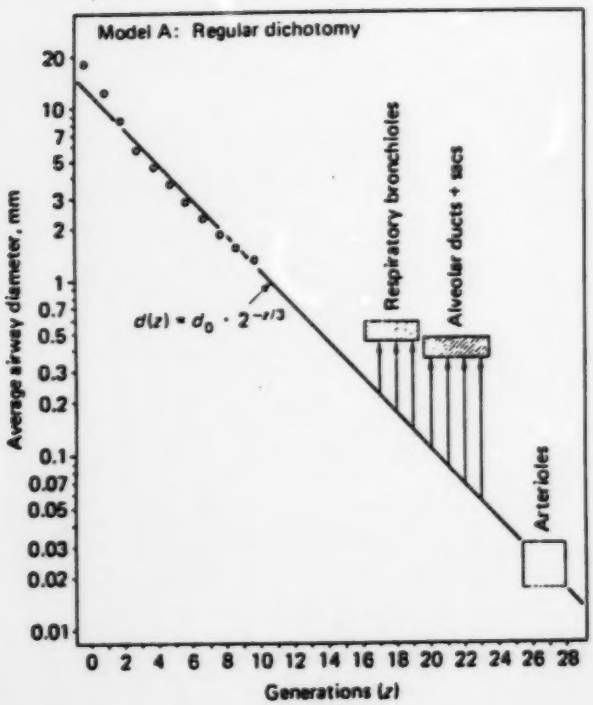

Figure 2 Average diameter of airways in human lung. (Weibel 1963)

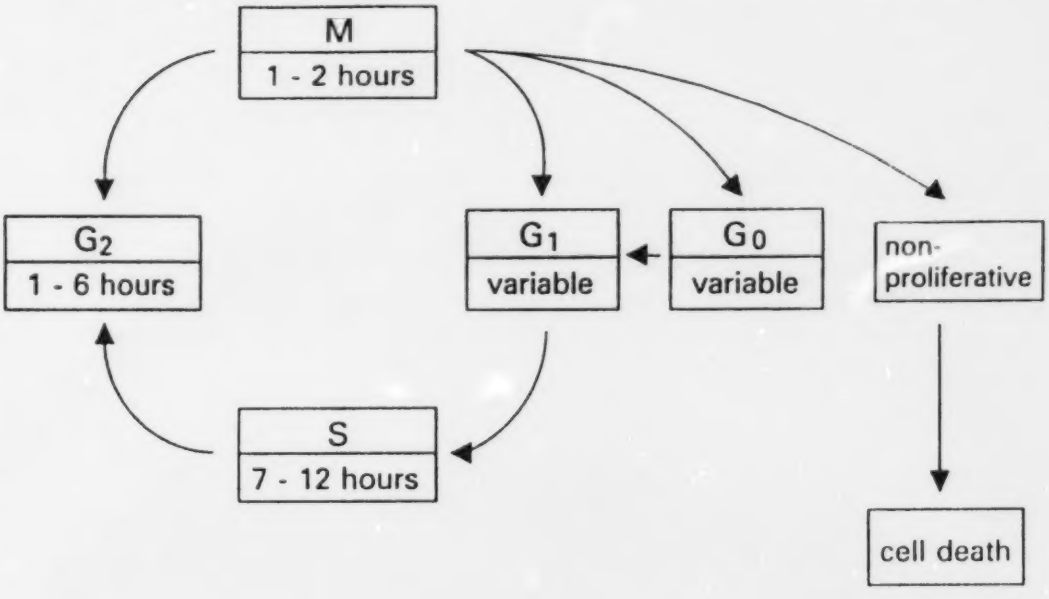

Figure 3 The cell cycle

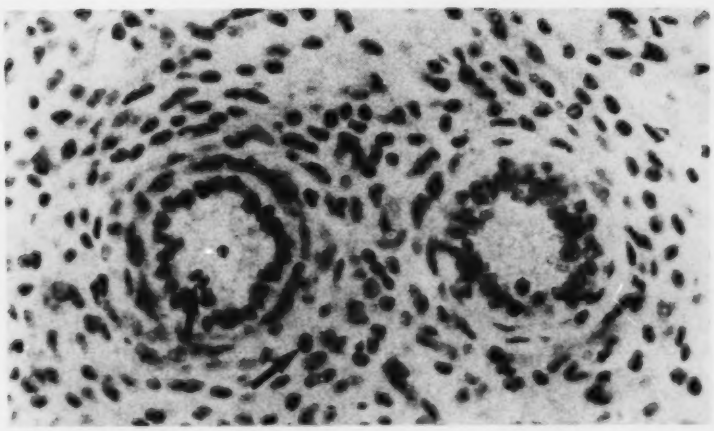

Figure 4 Foetal lung
Haematoxylin stain
arrows) mitotic figures

Most of the information we have about the phases of the mitotic cycle derives from animal studies. Cell labelling, for example, using tritiated thymidine though widely used in animals is not transferable to human studies. Until recently, measurement of proliferative activity in human tissue relied almost entirely upon the identification of mitotic figures in histologic sections (Figure 4).

There are several potential problems when mitoses are used as proliferative indicators in tissue. Mitotic figures can be difficult to identify with certainty and the process of mitosis may continue in unfixed tissue (Evans, 1926). Thus delayed placement of tissue in fixative may lead to an underestimation of the in vivo proliferating cell population, and differential penetration of tissue by fixative may influence regional variations in the proliferating cell populations.

Delay in fixation of tumors leads to an underestimation of the proliferating cell population (Graem and Helweg-Larsen, 1979). In primary breast carcinoma, where histological evaluation of mitotic activity is a component in the assessment of the grade of neoplasm, the number of mitoses declined by 43% when fixation was delayed for six hours (Start et al, 1991).

Cell turnover is low in the bronchial epithelium of rodents (Shorter et al, 1966; Bowden 1983) where it varies between eight to twenty-seven days in the rat and two to twenty-one days in the mouse. In recent years there have been a number of techniques developed which contribute to an understanding of human cell proliferation (Hall and Levison, 1990). Several involve assessing cell proliferation by detecting DNA synthesis during S phase (Figure 3) when the genetic information is doubled. Thymidine labelling and high resolution autoradiography have been the most favored tools for cell kinetic studies in animals, but the technique requires viable cells for uptake of tritiated thymidine and its incorporation into DNA during S phase; the necessity to radiolabel tissue in vivo or in vitro has limited its application in human studies.

The development of immunostaining provides a new method for the assessment of proliferation in human tissues. Some antibody techniques are more useful than others; the antibody C_5F_{10} which recognizes mitotic cells (Lloyd et al, 1985) has few advantages because it cross reacts with many other cellular components. Several immunologic markers are available for detecting S phase nuclei.

DNA synthesis in tissue can be assessed by detecting sites of incorporation of the thymidine analog bromodeoxyuridine demonstrated by specific antibody labelling, but BrdU must be incorporated by viable cells. In human studies, in vivo labelling is not usually possible and in vitro labelling is only successful

on small pieces of tissue which permit penetration of BrdU and its incorporation into nuclei. Only the outer 100 μm of tissue are reliably labelled; additionally thin slices may be difficult to cut without damaging the tissue.

Cells in S Phase can also be detected by a monoclonal antibody which recognizes DNA polymerase delta accessory protein, designated proliferating cell nuclear antigen (PCNA), in formalin fixed paraffin embedded sections (Galand et al, 1989; Hall and Levison, 1990; Waseem and Lane, 1990; Wood et al, 1990) PCNA antibodies have only recently become available commercially; the reliability and specificity of the technique and its application to human tissue has not been evaluated fully.

Preliminary evidence shows that labelling with PCNA antibody NCL-PCNA (Novacastra Laboratories, The Old Surgery, Queen Victoria Road, Newcastle upon tyne, NE14HL, England) and PCNA code M722 (Dakopatts A/S 42 Produktionsuej DK 2600, Glostrop, Denmark) may be variable, perhaps influenced by preservation of antigen by fixative. Cells from the periphery of sections which had more rapid access to fixative are more intensely and specifically labelled than areas further into the tissue where fixation was delayed; there may also be non-specificity of labeling because of antibody quality. PCNA techniques were not available until after completing this study of the proliferating cells in human bronchial epithelium.

The most extensively studied antibody which recognizes proliferative cells is Ki-67 which identifies a nuclear antigen, likely a component of the nuclear matrix (Verheijen et al, 1989 a & b), expressed in all phases of the cell cycle except Go (Gerdes et al, 1983, 1984) (Figure 3). There is a close correlation between Ki-67 immunoreactivity as an indicator of proliferation and measurements obtained by thymidine labelling, bromodeoxyuridine incorporation and flow cytometry (Hall and Levison, 1990). Ki-67 antibody has now been employed extensively in the identification of proliferating cells in many types of human tissue, particularly as as an operational marker for proliferation in neoplasia. There are, however, some potential inaccuracies in the use of Ki-67 for quantifying proliferation in neoplasia where cells may be nutritionally deprived. In experiments on nutritionally deprived cells there is a discrepancy between Ki-67 immunoreactivity and other methods of proliferative assessment (Sasaki et al, 1987; Walker and Camplejohn, 1986; Verheijen et al, 1989 b; Hall and Levison, 1990). A major limitation in the use of Ki-67 methodology has been the sensitivity of the antigen to chemical fixatives and the deterioration of antigenicity during storage of tissue, both of which may influence results. How the assessment of proliferative cell populations with Ki-67 antibody is influenced by short delays in freezing tissue after its excision is unknown, but bearing in mind that delay in fixing tissue may result in a substantial decline in mitotic figures (Start et al, 1991), only very fresh

material should be used for quantifying proliferative cell populations.

However despite these problems the Ki-67 technique offers the opportunity to identify cells at all stages of the proliferative cycle, potentially a distinct advantage in tissue such as bronchial epithelium where cell turnover is extremely low. In a morphometric study of the epithelium from all levels of the bronchial tree (Bowden and Baldwin, 1989; Baldwin et al, 1991) where multiple sections from more than 440 bronchi were examined, mitotic figures were extremely rare.

4. Objectives of the Study

1. Identify and enumerate the proliferating cells of the airways;
2. determine the proliferative capacity of the epithelial cells at different levels of the bronchial tree;
3. investigate the structure of the basal cells with reference to determining their involvement in the structural cohesiveness of the epithelium;
4. relate the information obtained from tasks 1, 2 and 3 to physiological parameters of importance to radiation dosimetry.

B. MATERIALS AND METHODS

1. Proliferating Cells in Control Tissue

Careful control of technique is imperative if the results of immunocytochemical investigations are to be valid. Initial experiments concentrated on the preservation of proliferating cell antigen and its demonstration in positive control tissue.

1.1. Materials

Fetal lung was selected as the control tissue for establishing the method because of the high incidence of proliferating cells in developing lung (Figure 4). Therapeutic abortion specimens, consisting of fresh unfixed fetuses of twelve to seventeen weeks gestation were used. The lungs were dissected, after routine pathological assessment of the fetus.

1.2. Methods

1.2.1. Freezing Technique: Numerous freezing and storage techniques were investigated to find the most appropriate procedure. Fresh, frozen tissue is best for the preservation of antigenicity (Hall and Levison, 1990). Blocks of fetal lung approximately 1 cm^3 were dropped separately into liquid nitrogen or frozen in saline in liquid nitrogen or in cryomolds in Tissue Tek OTC (Miles, Ames Division, Elkhart, Illinois), an embedding compound used routinely in histopathology laboratories for freezing and supporting tissue during microtomy. Different procedures for

storing frozen tissue were evaluated, and included storage in cryovials or aluminum foil in liquid nitrogen, or at -70°C or -20°C. The effects of different procedures on section quality and antigen preservation were examined.

Storage at -20° or higher temperature was unsatisfactory because of some antigen loss. Tissue snap frozen in liquid nitrogen and stored in liquid nitrogen, or -70°C, in an ultra deep freeze, produced satisfactory results. Antigenicity appeared to be relatively unaltered for up to four weeks, after which there was deterioration in staining intensity. Both antigenicity and tissue structure were affected adversely if the temperature of stored tissue blocks was raised to near the melting point before sectioning. The procedure adopted involved liquid nitrogen freezing of individual blocks and subsequent -70°C storage in cryovials or aluminum foil.

1.2.2. Sections: Detachment of sections during staining occurred frequently but was reduced if cryostat sections of 6-8 μm thickness were mounted on poly-L-lysine coated slides and air dried.

1.2.3. Fixation: It is generally agreed that for histological study 6-8 μm sections of snap frozen tissue are optimal for the preservation and demonstration of the antigen, but there is less agreement about fixation of cryostat sections. Acetone fixation followed by air drying has been widely preferred (Burger et al, 1986; Raymond et al, 1988; Sasaki et al, 1987), whilst acetone-petroleum ether has been advocated by others (Kamel et al, 1989). Buffered formalin has been considered to provide the best structural preservation of the antigen (Braun et al, 1988). Fixation with acetone-periodate-lysine-paraformaldehyde has been claimed to produce superior nuclear morphology (Hall et al, 1987) and preservation of proliferating cell antigen (Shepherd et al, 1988). After investigating the effects of all of the chemical fixatives above, it was determined that acetone fixation of fetal lung was compatible with the immunostaining techique employed subsequently.

1.2.4. Immunostaining: In order to determine the technique most suitable for our purposes, several different immunostaining procedures were used to demonstrate antibody location in fetal lung, as well as in breast and gastrointestinal tumors. The primary aim of this initial part of the study was to establish a procedure which stained sites of proliferating cell antigen intensely and without artefacts.

Proliferating cell antigen was demonstrated using as a guideline the procedure recommended by the manufacturer of the proliferating cell antibody Ki-67 (Dakopatts A/S42 Produktionsuej DK-2600 Glostrup, Denmark). Air dried, acetone fixed cryostat sections on poly-L-lysine coated slides were incubated in a moist chamber at room temperature in antibody Ki-67, washed in tris buffered saline (TBS) and incubated in a moist chamber at room temperature in anti-

mouse immunoglobulin. Optimal times were achieved by experimentation. Following a further wash in TBS, sites of proliferating cell antigen were demonstrated. Avidin-biotin-peroxidase (Hsu et al, 1981; Hsu and Raine, 1984; Shepherd et al, 1988; Raymond 1988) methods were employed using different substrates; a range of dilutions were tested. The alkaline phosphatase anti-alkaline phosphatase (APAAP) technique (Cordell et al, 1984; Gatter et al, 1986) was also used to detect Ki-67 labelling and proved to be superior to peroxidase methods. Fast red TR salt and new fuchsin (NF) were employed as substrates, at different dilutions. The APAAP technique, using NF as substrate, was preferred because it was free of background artefacts. Sections were incubated in APAAP complex (Dakopatts code number D651) at room temperature in a moist chamber, and washed in TBS before the alkaline phosphatase substrate was added at room temperature. In all preparations endogenous alkaline phosphatase was blocked with levamisole. Following a wash in phosphate buffered saline, sections were counterstained with hematoxylin and mounted in aqueous mounting medium. The staining of sites of proliferating cell antigen was enhanced by repeating the anti-mouse immunoglobulin and subsequent steps, before adding the alkaline phosphatase substrate.

Sites of proliferating cell antigen were bright red and contrasted well with the hematoxylin nuclear stain. In fetal lung nuclear staining was clearly specific (Figure 5). When tris buffer was substituted for the monoclonal antibody, fetal lung reactions showed no staining with the APAAP technique. Thus the ground work was laid for application of the Ki-67 technique to adult bronchial epithelium.

Demonstration of S Phase was explored using the thymidine analog 5 bromodeoxyuridine (BrdU), which is incorporated into replicating DNA during S Phase and located subsequently by detecting immunochemically, cells which exhibit an antibody specifically directed against BrdU (Schutte et al, 1987a, b). The procedures used were those outlined by Amersham International plc (Amersham England) and Eurodiagnostics BV (Postbox 2820, 7203 GC, Apeldoorn, The Netherlands). Optimal dilutions and times were achieved by experimentation.

Small pieces (1 X 2 mm) of fresh fetal lung, breast and gastrointestinal tumors with a high proliferating cell content were incubated in diluted BrdU preheated to 37°C before use. After washing in phosphate buffered saline (PBS) at 37°C, each specimen was fixed in 10% neutral buffered formalin and processed to paraffin. 4 μm sections from within 100 μm of the surface exposed to labeling were mounted on coated slides and dried. Sections were cleared of paraffin wax and rehydrated. After blocking of endogenous peroxidase activity and pepsin treatment, sections were incubated in diluted anti-BrdU antibody at 37°C. Following washing with PBS, sections were incubated at room temperature in diluted anti-mouse immunoglobulin. Washing in PBS was followed by immersion in diaminobenzidine solution. Sections were washed in

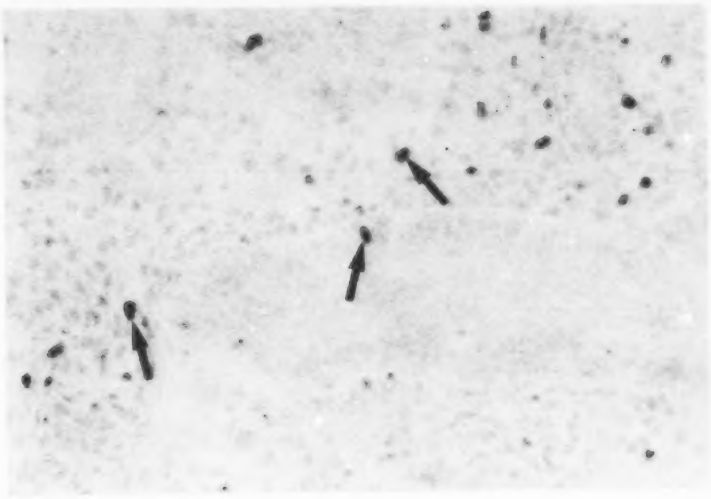

Figure 5 Foetal lung
Ki-67 technique
arrows) labelled nuclei

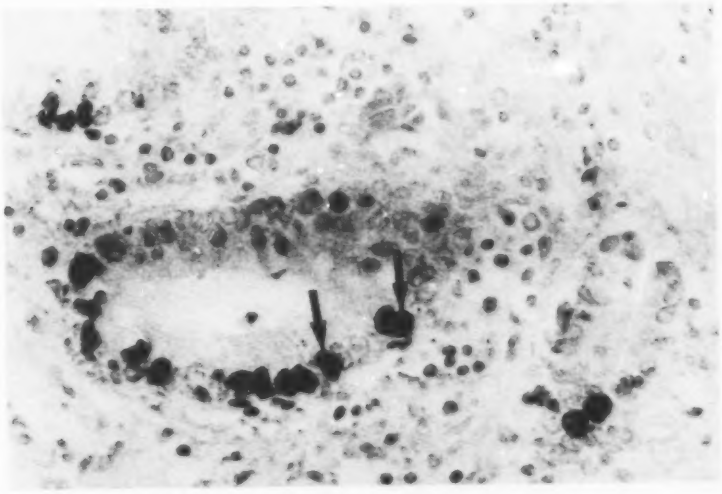

Figure 6 Tumor
Brd U technique
arrows) labelled nuclei

distilled water, weakly stained with either a nuclear or cytoplasmic counterstain, dehydrated, cleared and mounted. The technique was effective in demonstrating S Phase nuclei (Figure 6), but only reliably in sections from the outer zones of small pieces of tissue optimally exposed to the antibody procedure. The results on sections from deeper in the blocks were variable. The technique was applied to small tissue slices containing bronchial epithelium, however there were a number of technical difficulties encountered. It was difficult to cut slices sufficiently thin to ensure the structural integrity of the lung tissue. A great number of tissue slices were rejected for a variety of reasons, but damage and plane of section were the most prominent. Whilst the technique is undoubtedly useful for demonstrating S Phase cells, its value for quantifying proliferating cells in bronchial epithelium is questionable because of technical difficulties outlined above. The technique was less suitable than Ki-67 for the survey of proliferative capacity of the bronchial epithelium.

2. Proliferating cells in adult epithelium

2.1 Materials

Lung specimens from the morning surgical list were dissected within three hours of their excision. Specimens which were not available for many hours were not used in the study. Blocks containing bronchi were dissected from a total of nineteen selected surgical lung specimens. Samples for proliferating cell assessment were from seven cases as follows.

Histopathology Diagnosis	Number	Male	Female
Squamous Carcinoma	1	1	
Adenocarcinoma	4	1	3
Large Cell Carcinoma	2	1	1
Total	7		

Smoking and occupational history of each patient and surgical pathology reports were recorded.

Histopathology Diagnosis	Male	Female	Smoking History pack years	years quit
Squamous Carcinoma	X			23
Adenocarcinoma		X		30
"		X	50	
"		X	40	
"	X		45	
Large Cell Carcinoma		X	40	
"	X			4

2.2 Methods

Multiple samples of each lung specimen containing bronchi were dissected from areas remote from those with pathological appearances. From these samples, 81 different bronchi were selected for measurement and preparation of multiple stained sections.

2.2.1. Freezing technique: Each tissue block, approximately 1 cm^3, was quenched in liquid nitrogen and stored in cryovials or aluminum foil at -70°C, as outlined previously. Fetal lung positive control tissue was prepared identically.

2.2.2. Fixation and processing for light microscopy: Tissue blocks from six specimens were fixed in 10% neutral buffered formalin and methacarn, processed and embedded in paraffin.

2.2.3. Fixation and processing for electron microscopy: From three lung specimens, tissue blocks no larger than 2 mm X 2 mm X 0.5 mm were dissected from cross sections of bronchi measured under a microscope, fixed in 4% phosphate buffered glutaraldehyde pH 6.8, processed and embedded in Epon-Araldite. Blocks of bronchial gland were also processed. Sections of glutaraldehyde perfused lung tissue blocks, prepared for a previous study (Bowden and Baldwin, 1989), were also used in the study of basal cells. 0.5 μm sections, from a range of bronchi from Generation 4 - Generation 12 and bronchial glands, were stained with toluidine blue. Ultrathin sections with silver-gray interference color were stained with uranyl acetate and lead citrate, and examined in a Zeiss 10 CR electron microscope.

2.2.4. Ki-67 immunostaining: Blocks were oriented to enable bronchi to be cut in cross section; in many instances because small airways are difficult to see in fresh lung, cross sections were achieved only by cutting many blocks. 8 μm cryostat sections of bronchi were mounted on poly-L-lysine coated slides and air dried. Controls were used to verify reproducibility of the technique. Sections of fetal lung, known to contain many proliferating cells, were prepared identically for use as positive controls. In earlier experiments acetone fixation of air-dried sections gave optimal Ki-67 staining of proliferating cells in fetal lung; the same procedure was adopted initially for both adult bronchi and fetal lung. However, acetone fixation proved to be unsatisfactory for adult lung because of an unexpected cytoplasmic cross-reaction of the immunostain (Figure 7), principally, but not exclusively in basal cells. The cross reaction was presumably with cytoplasmic cytokeratin. There was no cytoplasmic staining of cells in bronchial lymphoid tissue immunostained with Ki-67 (Figure 8). After much experimentation the fixation protocol was altered to five seconds fixation in 10% neutral buffered formalin to improve the specificity of the Ki-67 immunostaining.

Figure 7 Bronchial epithelium
Ki-67 technique
arrows) non-specific staining of basal cell cytoplasm

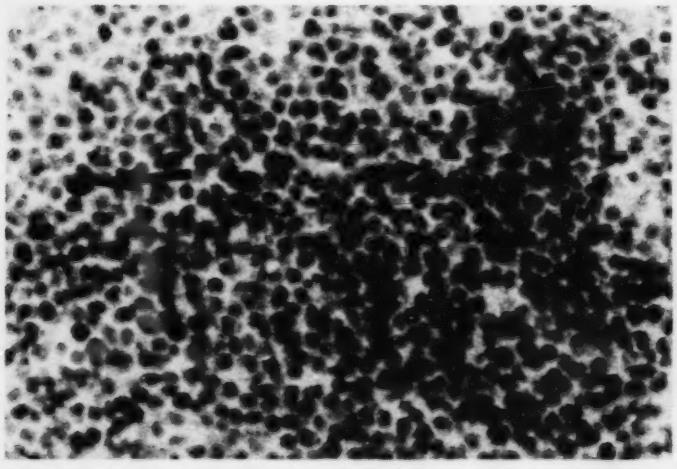

Figure 8 Bronchial lymphoid tissue from same preparation as Figure 7
Ki-67 technique
arrows) labelled nuclei

Fixed, air-dried sections were stained using the Ki-67 monoclonal antibody APAAP technique established in preliminary experiments for demonstrating proliferating cells in fetal lung. Each batch of Ki-67 test sections of adult bronchial epithelium was accompanied by a section of bronchial epithelium in which tris buffer was substituted for the Ki-67 antibody. Sections of fetal lung which accompanied adult lung test sections acted as positive controls for the Ki-67 technique; bronchial lymphoid tissue when present in bronchial epithelium test slides also acted as a positive control.

2.2.5. BrdU immunostaining: The technique used for the demonstration of cells at S phase was identical to that used in preliminary experiments. Results on bronchial epithelium were unreliable because of the technical difficulties explained previously (see 1.2.4.).

2.3. Morphometry

2.3.1. Selection of Bronchi: Bronchi were selected for measurement and counting only if the orientation of the epithelial cells on the basement membrane indicated clearly that both were cut in cross section and that technical quality was optimal.

2.3.2. Measurement of Bronchi: A microprojector consisting of a Leitz microscope fitted with X 2.5, X 25, and X 40 objectives, a prismatic projection head and a high intensity light source (XM-150 Kramer Scientific Corporation) were used to project a micrometer scale onto a sheet of paper. The magnified scale was measured and the total magnification for each objective calculated. Once the magnification factors were established, the location of the microprojector was fixed to ensure a constant focal length. The calibration was checked regularly. A stained section of bronchus was projected onto a sheet of paper. The image of the lumen was then traced in ink and the magnification recorded. Subsequently the drawing was traced with a cursor on a tablet in a MOP Videoplan Image Analysis System (Carl Zeiss, Oberkochen, Germany) and the diameter of the airway computed from the circumferential measurement, by using a standard d-circle measuring program (Kontron Bildanalyse GMBH, Breslauer Strasse 2, D-8057, Eching, Munich, Germany).

2.3.3. MOP Videoplan Image Analysis System: The MOP Videoplan Image Analysis Computer System is designed for data acquisition and computation of geometric characteristics by tracing structures of images placed on a measuring tablet. The basic units are a control microcomputer, monitor, keyboard and digitizer tablet and printer. The computer has a 64K byte system memory and 16K byte memory for representation of graphics and alpha numerics on a monitor. A 20 M byte hard disk is divided into four drives, each with a capacity of 5 M bytes; a floppy disk drive with a capacity of 580K bytes completes the computer system. Co-ordinate data is generated on

the tablet and is continuously calculated into freely selected geometric parameters by the computer. An integrated dual floppy disk drive is utilized for program and data storage. The standard measurement programs and measurement data are stored separately on hard disks. The standard measurement program Y-1/Y-2 accommodates a parameter display consisting of several different functions with a range of measurements from area type definitions (circumscript of structures), one of which, the d-circle (which computes the diameter of an equivalent circle from a measured area) was used to establish the diameter of airways.

2.3.4. Cell Enumeration: In multiple cross sections of each bronchus of computed diameter and Weibel generation (Weibel, 1963) the number of cells positively immunostained with the Ki-67 technique were counted, and classified according to their morphology as typical basal cells, atypical basal cells and columnar cells (Figure 1). Cell enumeration for proliferating population assessment was conducted only on sections free of hyperplasia and metaplasia. The total number of typical basal cells and atypical basal cells were also counted in multiple sections. From cell counts and circumscript measurements the average number of proliferating typical and atypical basal cells, and columnar cells, per mm of epithelium in cross sections of bronchi of different diameter and generation were calculated. The number of different proliferating cells were calculated for a 1 mm length of each bronchus. Based on the assumptions that labelled cells were present throughout each bronchial generation and each section was 8 μm thick, the number of labelled cells was multiplied by 125 to obtain the population/mm.

The proportion of typical and atypical cells in the proliferating cycle in each bronchus of different diameter and generation was expressed as a percentage.

2.4. Statistical Methods

Means, standard error, and standard deviation, by generation and cell type, were computed for normal distribution. Analysis of variance was performed on an Amdahl-4700 computer using a biomedical data package (BMDP version 5.2, BMDP Statistical Software Incorporated, Los Angeles, California). Assistance with statistical analysis was provided by the Division of Biomedical Statistics, University of Manitoba.

C. RESULTS

1. Detection of Proliferating Cells in Control Tissue
Ki-67 Antibody

Proliferating cell antigen sites were revealed in acetone fixed frozen sections of fetal lung (Figure 5), and breast and gastrointestinal tumors, with both immunoperoxidase and alkaline

phosphatase anti alkaline phosphatase (APAAP) techniques. APAAP using new fuchsin as substrate proved superior because antigen sites were bright red, enabling distinction from unlabelled nuclei which were stained lightly with hematoxylin. Negative control slides were unlabelled. With the APAAP new fuchsin technique there was none of the fine granular background staining experienced when the fast red TR salt was used as substrate. Examination of sections of fetal lung stored frozen for many weeks, showed that there was deterioration in the intensity of antigen staining. For up to four weeks in frozen storage there appeared to be no change in immunostaining intensity.

2. Detection of Proliferating Cells in Adult Lung
Ki-67 Antibody

When the Ki-67-APAAP technique was applied to sections of adult lung prepared identically to the fetal lung control tissue, sites of proliferative activity were stained, but the cytoplasm of basal cells was also stained (Figure 7). It was not possible to distinguish nuclear labelling, and the task of counting and enumerating labelled nuclei in basal cells could not be conducted. The cytoplasm of most but not all other epithelial cells was unstained. Nuclei of proliferating cells in bronchial lymphoid tissue in the same sections were labelled specifically. In negative controls, that is sections which received no Ki-67 antibody but were otherwise treated identically, there was neither nuclear nor cytoplasmic staining. The results of Ki-67 immunoperoxidase tests were equivalent to Ki-67 APAAP results.

Cross-reaction of Ki-67 antibody with cytoplasm has only been reported previously in the epidermis, so that the cross reaction with cytoplasm in bronchial epithelium was unexpected. From experiments undertaken to determine the best procedure to preserve the antigen, it was evident that antigen preservation by freezing, the fixative used, and fixation duration were critical. Reduction of unwanted cytoplasmic staining was achieved only if air dried cryostat sections were fixed for five seconds in 10% neutral buffered formalin. Where cross reactive cytoplasmic staining was pale or almost absent labelled nuclei could be identified (Figures 9-10); but frequently cytoplasmic staining was too intense to differentiate a stained nucleus. At the outset of this investigation bronchi were dissected from lobes of several different lungs and frozen. When the improved antigen preservation technique, which was successful on recently harvested lung, was applied to sections from stored material, proliferating cells were not demonstrable. There have been conflicting reports of proliferating cell antigen preservation by freezing. Antigenicity has claimed to be preserved for periods ranging from a few weeks to months, but it is evident from this experience that the antigen does not survive more than a few weeks in frozen storage.

Stored tissue from the early cases, which included a full range of bronchial generations, was discarded because of antigen deterioration. New tissue was collected. Unfortunately for the purpose of this study, there was a change in the surgical protocol whereby lobectomy or pneumonectomy was indicated only where there were large lesions or disseminated pathology. Such specimens were

Figure 9 Bronchial epithelium
Ki-67 technique
arrow) labelled basal cell nucleus

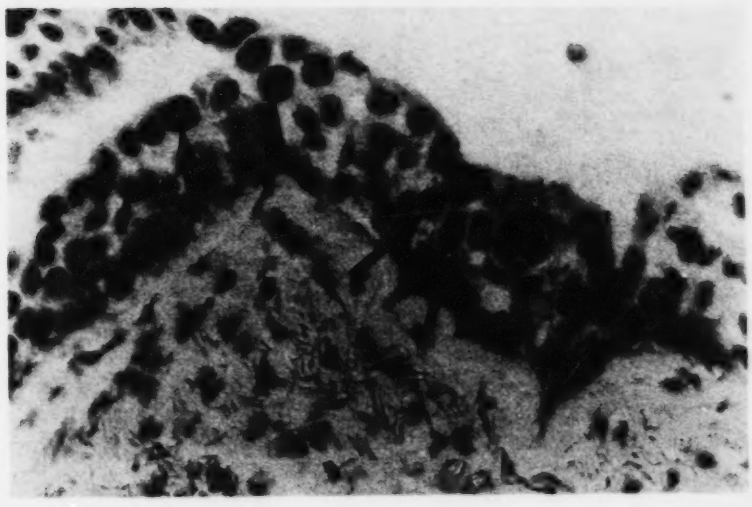

Figure 10 Metaplastic bronchial epithelium
Ki-67 technique
arrows) labelled nuclei

unsuitable and the supply of "clean" lobes with small lesions of the type used in the previous study on epithelial measurement (Bowden and Baldwin, 1989, Baldwin et al, 1991), were no longer available. At the Health Sciences Centre there is now an established preference for the surgical removal of wedges of lung if they contain small lesions. Such lung wedges are stapled extensively, so that even if they contain larger airways, they are so damaged as to be useless for study. Only smaller airways remain undamaged and suitable for analysis. This change in protocol limited severely the availability of material for the study. The lung samples used represent only a small proportion of the total number of samples dissected and sectioned. Many entire cases were excluded because of pre-existing clinical conditions or because of pathological change. In two instances all tissues were lost to the study so that they could be examined for a diagnostic lesion. A large number of tissue blocks and multiple sections for each specimen could not be used because of inappropriate plane of section, technical quality of sections, stain specificity, or because of epithelial alteration (i.e. hyperplasia, metaplasia). The sections on which enumeration of labelled cells was possible represent only a small proportion of the total number of bronchial sections immunolabelled. Despite careful preparation, in many instances cytoplasmic staining prevented recognition of nuclear labelling, although nuclear labelling in adjacent areas of the section was optimal: for example in bronchial lymphoid tissue.

Of a total of eighty-one bronchi from which multiple sections were prepared, only material from twenty-eight bronchi from seven cases were suitable for labelled cell enumeration.

All sections were examined using X 100 oil immersion optics. Ki-67 labelled typical and atypical cells, and columnar cells, were identified and enumerated in multiple cross-sections of each bronchus (Table 1). The total population of both types of basal cells was also enumerated. Means and standard deviations were determined. The diameter of each bronchus was computed and sorted according to generation (Weibel, 1963). The population of labelled basal cells of both types were calculated for each mm of epithelium for bronchi of different diameters and generations. Total basal cells for each mm of epithelium in sections was calculated, and means and standard errors determined for different types of labelled and unlabelled cells for each generation (Table 2).

These data were subjected to analysis of variance (Tables 3A,3B); because there was a wide range of values for each group the data were also transformed logarithmically.

The percentage of basal cells labelled was calculated for each bronchus examined (Table 4A). Bronchi were sorted according to generation, and means and standard errors expressed. The percentages of labelled basal cells were subjected to analysis of variance (Table 4B).

No significant differences ($p=<0.05$) were revealed by analysis of variance in the population of labelled typical or atypical basal

cells/mm epithelium (Table 3A), or total typical and atypical basal cells in different bronchial generations (Table 3B). Logarithmic transformations suggest the underlying distributions are "lognormal".

Calculations from data in Table 2 revealed the mean population of proliferating cells in a mm length of each bronchus (Table 5A) and for each bronchial generation (Table 5B). The study included some patients with a long history of heavy smoking (40-50 pack years) and others who had ceased smoking many years previously (23-30 years). From data of numbers of labelled cells and total basal cells/mm epithelium in cross sections of bronchi, means and standard errors were sorted according to bronchial generations, and subjected to an analysis of variance (Tables 6A, 6B).

In all bronchial generations there were significant differences in the populations of labelled basal cells/mm between former smokers and smokers (Table 6A). In former smokers there were more proliferating typical basal cells ($P = 0.006$) and atypical basal cells ($P = 0.002$).

In generations 12 - 15 the populations of proliferating columnar cells/mm epithelium were signficantly different between former smokers and smokers ($P = 0.001$) (Table 6A).

Between former smokers and smokers there were significant differences in the populations of labelled basal cells/mm epithelium between generations 7 - 9 and generations 12 - 15 of the bronchial tree (total basal cells $P = 0.01$, atypical basal cells $P = 0.014$, typical basal cells $P = 0.054$) (Table 6A).

Between generations 7 - 9 and 12 - 15 in former smokers there were significant differences in the numbers of basal cells/mm epithelium (typical basal cells $P = 0.007$) and there were also significant differences between generations 7 - 9 and generations 12 - 15 in former smokers and smokers (atypical basal cells $P = 0.02$) (Table 6B).

In generations 7 - 9 there was a significant difference between former smokers and smokers in the percentages of labelled typical basal cells in the proliferating basal cell population ($P = 0.02$) (Table 6C).

3. Basal Cell Morphology

Recently two types of basal cells have been identified throughout the adult human bronchial tree (Bowden and Baldwin, 1989; Baldwin et al, 1991): the typical pyramidal cell and an atypical elongated cell distributed circumferentially (Figure 11). Both cell types have also been recognised in hamster trachea (McDowell et al, 1983) and bronchi (Breuer et al, 1990).

The basal cell of human respiratory epithelium is characterized as a small pyramidal element which is attached to the basal lamina; but the cell apex does not reach the luminal surface of the epithelium (Jeffery and Reid, 1973, 1975, 1977, McDowell and Beals,

Figure 11 Bronchial epithelium
a) atypical basal cell
b) typical basal cell

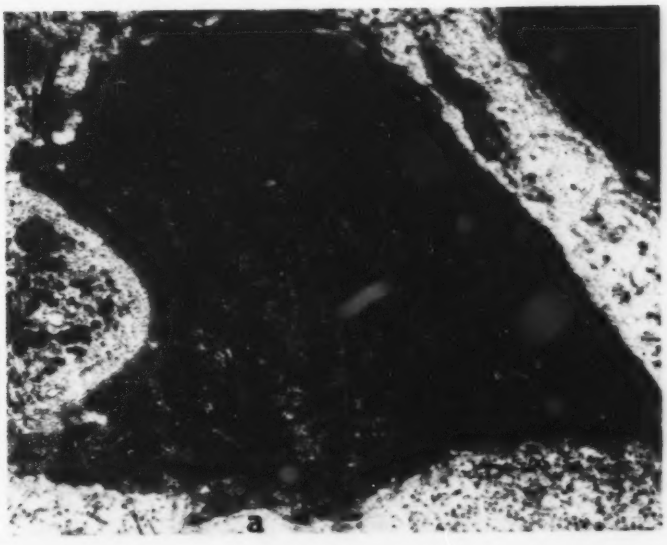

Figure 12 Typical basal cell
a) basement membrane
arrow) desmosome

Figure 13 Atypical basal cell and columnar cell.
a) atypical basal cell
b) desmosomes
c) columnar cells
arrows) hemidesmosomes

1986). Basal cells are usually separated from one another by the cytoplasm of columnar cells, but sometimes form a continuous layer. In human bronchial epithelium there may be more than one layer of basal cells (McDowell and Beals, 1986).

Using the electron microscope, the typical basal cell (Figure 12) was observed to have a high nuclear:cytoplasmic ratio, and organelles were relatively sparse. The cells were attached to the underlying basal lamina by hemidesmosomes; desmosomes were at interfaces with columnar cells. Bundles of filaments were distributed randomly and some terminated at junctions.

The atypical basal cell nucleus was spindle shaped. The cytoplasm was predominantly polar in distribution (Figures 13, 14, 15) and extended into processes which coursed along the basal lamina, beneath and between the cytoplasm of columnar cells (Figure 16). The cytoplasm (Figure 15) was of moderate density. The organelles included small, oval mitochondria, some rough endoplasmic reticulum and variable quantities of polyribosomes, which were frequently abundant. Golgi profiles were seen occasionally and lysosomes were present. Larger electron lucent droplets with granular components at the periphery were found in the polar cytoplasm of many cells. Small cytoplasmic vesicles were sometimes present, as were pinocytotic vesicles on the basal surface (Figures 15, 17, 18). Filaments, approximately 10 nm in diameter, were mostly in bundles (Figure 15, 17) and aligned with the longitudinal axis of the cell, but some were distributed randomly (Figure 18). In some cells the bulk of the cytoplasm was packed with filaments. Desmosomes were present where atypical basal cells contacted columnar cells (Figures 13, 19) and where atypical basal cell processes contacted one another (Figures 14, 20, 21) or where perikaryal cytoplasm was apposed (Figure 22). Interdigitations, in addition to desmosomes, were present between contacting cytoplasmic processes of atypical basal cells (Figure 22) and between atypical and typical basal cells, where they were present as a double layer (Figure 23). Columnar cells were attached to one another by desmosomes (Figures 13, 16), but there were no hemidesmosomes or other recognisable means of attachment between columnar cells and the basal lamina (Figure 16).

The different morphology of the two types of basal cells was maintained throughout the bronchial tree examined, and there were no morphological differences within each population. There were fewer junctional attachments between typical basal cells and adjacent columnar cells (Figure 12) than there were between atypical basal cells and columnar cells (Figure 19); but there was no obvious variation in the number of junctions between atypical cells and columnar cells in different generations of the bronchial tree.

It has been noted previously that the appearance of atypical basal cells was reminiscent of myoepithelial cells (Bowden and Baldwin

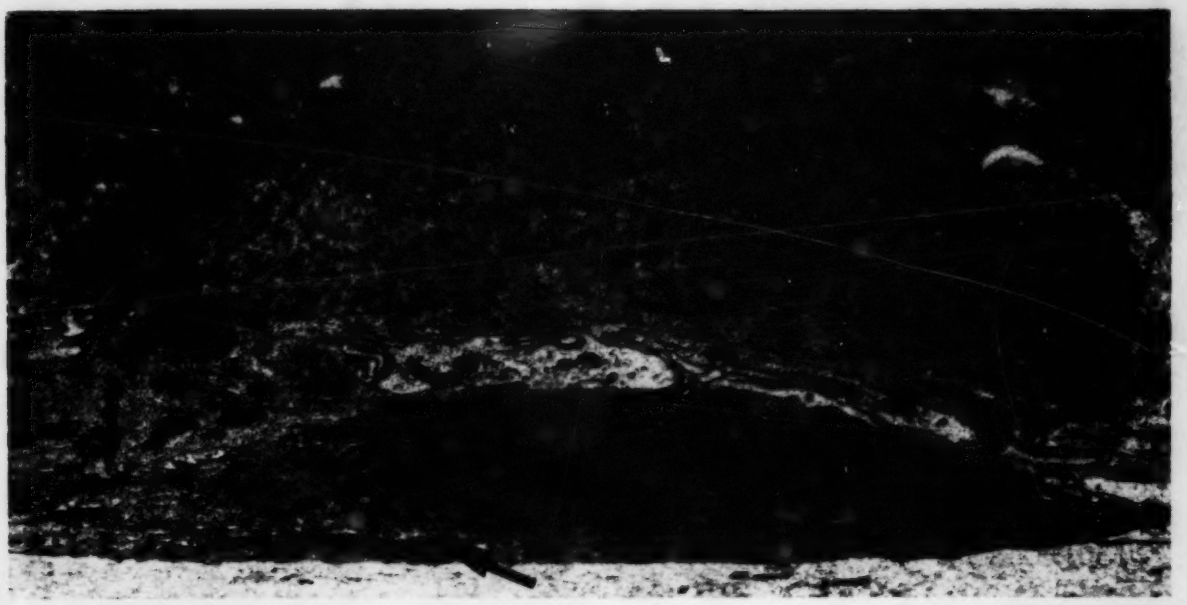

Figure 14 Atypical basal cell and columnar cells.
a) atypical basal cell
b) columnar cells
arrows) desmosomes

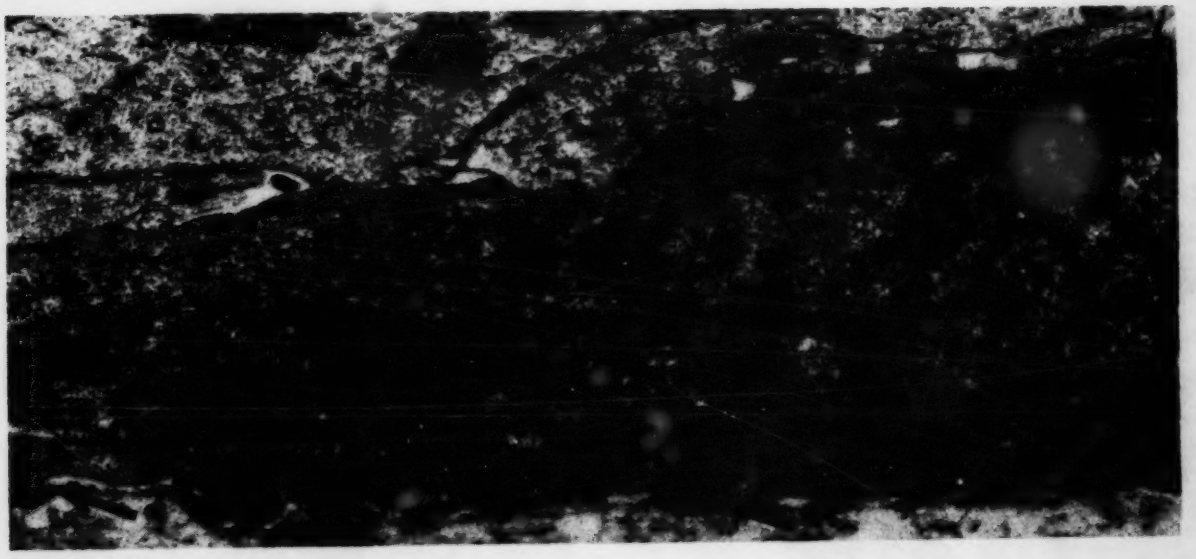

Figure 15 Atypical basal cell
a) endoplasmic reticulum
b) polyribosomes
c) Golgi
d) lysosome
e) mitochondrion
f) filaments
g) lipoprotein
arrows) hemidesmosomes

Figure 16 Atypical basal cell and columnar cells.
a) atypical basal cell processes
b) columnar cells
c) desmosome
d) basement membrane
arrows) hemidesmosomes

Figure 17

Atypical basal cell cytoplasm
a) filaments
b) basement membrane
arrows) pinocytosis vesicles

Figure 18

Figure 19 Atypical basal cell
a) basement membrane
arrows) desmosomes

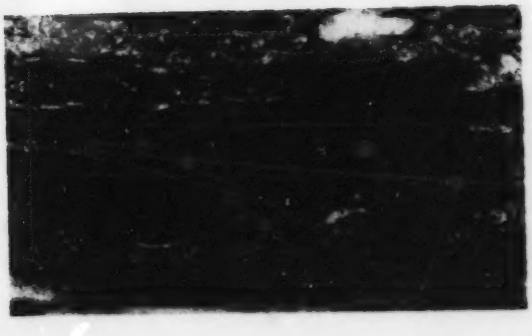

Figure 20

Contacts between atypical basal cells
arrows) desmosomes

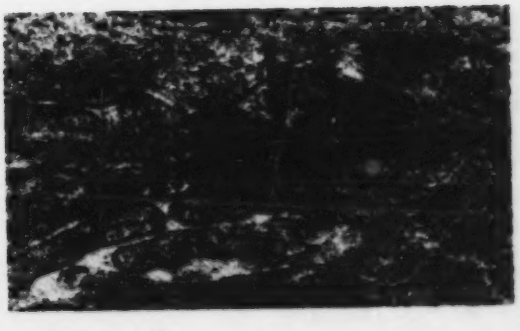

Figure 21

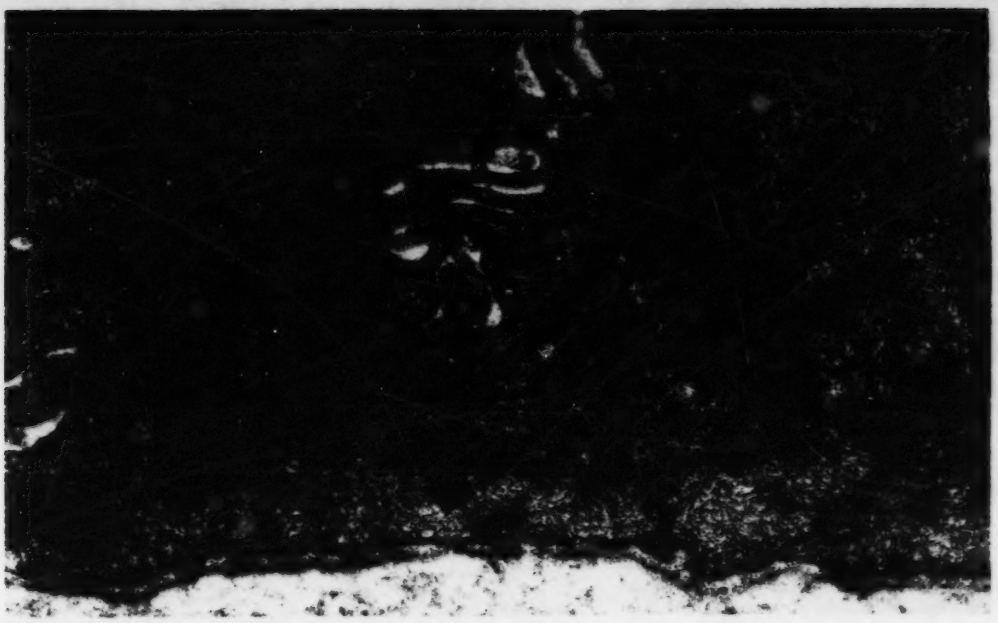

Figure 22 Contacts between basal cells
a) cytoplasmic interdigitations
arrows) desmosomes

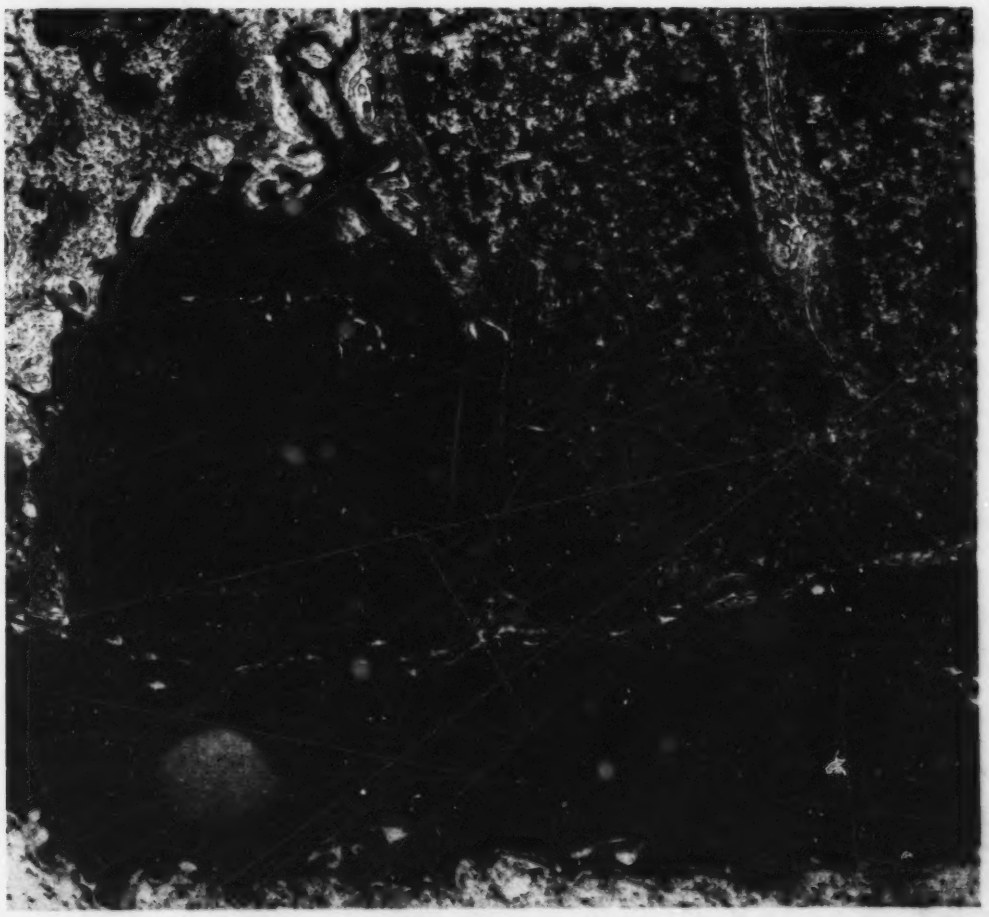

Figure 23 Basal cells present as two layers of cells.
a) atypical basal cell
b) typical basal cell
c) columnar cells
arrows) desmosomes

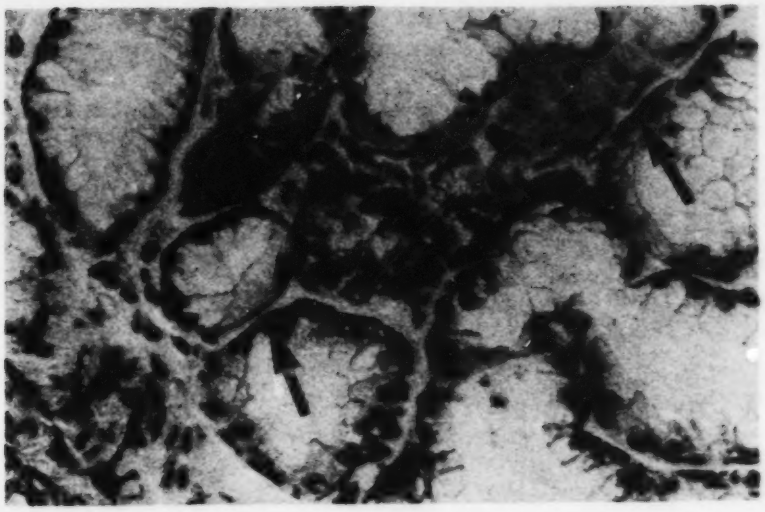

Figure 24 Bronchial gland
α - actin technique
arrows) positive reaction in myoepithelial cells

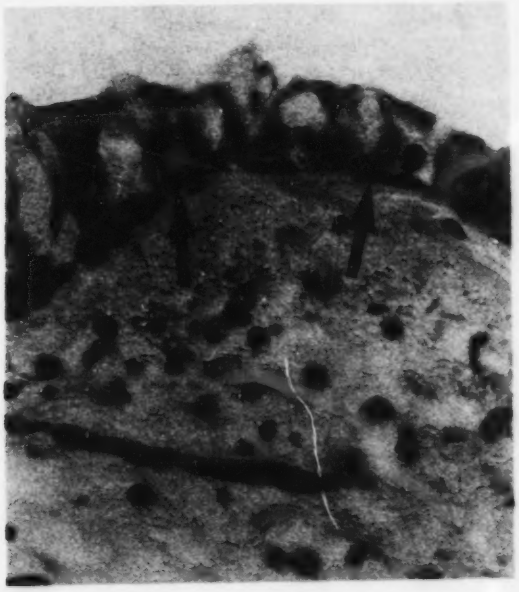

Figure 25 Bronchial epithelium
α - actin technique
arrows) negative reaction in basal cells
a) positive reaction in smooth muscle

Figure 26 Myoepithelial cell
a) cytoplasm of secretory cell
arrows) basement membrane.

Figure 27 Myoepithelial cell cytoplasm
a) lipofuscin
b) filaments
c) filament densities
d) pinocytosis vesicles
arrows) basement membrane

1989). Immunocytochemistry and ultrastructural comparisons between myoepithelial cells in bronchial glands and atypical basal cells in bronchial epithelium revealed their different nature. The cytoplasm of myoepithelial cells, known to contain contractile filaments, reacted positively for muscle specific α-actin (Figure 24); whilst α-actin was absent from the cytoplasm of basal cells (Figure 25). Myoepithelial cells are rarely connected to other cells of the epithelium. The myoepithelial cell (Figure 26) possessed an elongated nucleus which was located centrally; organelles were mostly restricted to the perinuclear region, but some cytoplasmic organelles were interspersed between the masses of filaments. Pinocytosis vesicles were on the basal surface and lipofuscin was present (Figure 27). The cytoplasm basal to the nucleus, and the processes of the cells, were laden with masses of parallel 6 nm filaments, which were distributed exclusively along the longitudinal access of the cell (Figures 26, 27) and contrasted with the filaments and their arrangement in the basal cells (Figures 15, 17, 18). At nodal points in the filaments of myoepithelial cells there were elongated aggregations of moderately dense amorphous material (Figures 26, 27). Some filaments terminated at dense plaques on the plasma membrane. These features, which are consistent with myofilament arrangement in contractile cells, were absent from basal cells.

4. <u>Basal Cell Morphometry</u>

From data generated during the previous study of the thickness of bronchial epithelium (Bowden and Baldwin, 1989, Baldwin et al, 1991,) measurements of the distances from the lumenal surface of the epithelium to the nucleus of basal cells, and thickness of adjacent epithelium (Figure 28), showed that both measurements were less for atypical than for typical basal cells. Furthermore there were significant differences between bronchial generations ($p = < 0.05$) (Table 7). The distances from the tip of the cilia to the basal cell nucleus were also less for atypical cells.

The thickness (Figure 28) of the nucleus of atypical basal cells varied very little throughout the bronchial tree (3.11 μm Generation 1, 2.79 μm Generations 7-16), but was less than that for the nucleus of typical basal cells, which also showed little variation in different bronchial generations (4.71 μm Generation 1, 4.26 μm Generations 7-16) (Table 7).

Atypical cell nuclei were consistently closer to the lumenal surface because of the lesser thickness of epithelium overlying atypical basal cells (Figure 29).

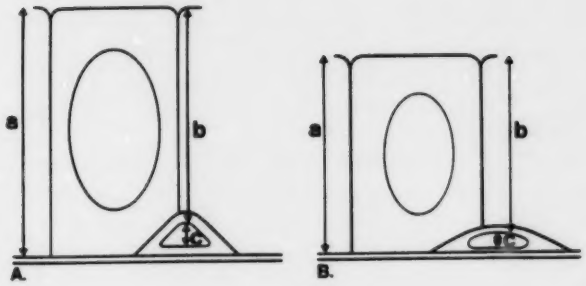

Figure 28 Epithelial and basal cell measurements
A typical basal cell
B atypical basal cell
a) epithelial thickness
b) lumenal surface of epithelium to basal cell nucleus
c) nuclear thickness

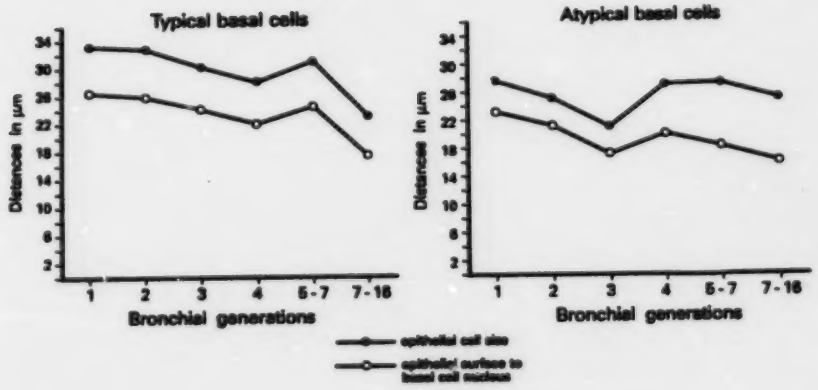

Figure 29 Distances: lumenal surface to basal cell nucleus, and adjacent epithelium

D. DISCUSSION

Most of what is known about proliferating cell populations in bronchial epithelium has been derived from studies of experimental animals, usually small rodents. The majority of these reports gives figures for mitotic activity only and, whilst it appears that basal cells and secretory cells may play a proliferative role, there is some species variation. (Ayers and Jeffery, 1988).

In general, proliferative activity in the respiratory tract is low. Data from rodents (Ayers and Jeffery, 1988) show the number of cells entering mitosis per hour per thousand cells (i.e. REM) is 0.15 - 0.4 for bronchial epithelium and 0.16 - 3 for trachea. For comparison the REM for rodent duodenal epithelium is 30. The percentage of cells in mitosis at any one time is the mitotic index (MI). This varies with airway level, animal strain, sex and age, and decreases from trachea to distal airways in young animals. This trend is less pronounced in older animals. Diurnal variations in mitotic index and labelling index, as measured by uptake of tritiated thymidine, have been demonstrated in various tissues. In the respiratory tract, a morning peak has been found in rats (Messier and LeBlond, 1960; Romanova, 1966; Sokolova, 1975) and an afternoon/evening peak in mice and hamsters (Koburg, 1962; Kmoch et al, 1975; Das et al, 1979).

We know much less about cellular proliferation in the human lung. The basal cell of the tracheo-bronchial tree is generally considered to be the progenitor of all bronchial epithelial cells and, therefore, the cell most likely to be at risk from carcinogenic agents. Much less attention has been given to the other cells of the bronchi and their potential for neoplastic transformation.

There is an increased incidence of lung cancer in uranium miners and, in common with other occupationally related cancers of the lung, smoking is thought to exert a greater than additive effect (BEIR III, 1980; Sevc et al, 1988). There might be a multiplicative interaction between the effects of inhaled radioactive material and cigarette smoking (ICRP, 1987; BEIR IV, 1988). Lung carcinogenesis in uranium miners is believed to be related to uranium decay with the production of Rn daughters which may attach to molecules of water vapor or dust particles as "cluster ions" (Chamberlain and Dyson, 1956). The mean radioactive diameter of these clusters is 0.25 μm in non-operational mines and 0.4 μm in operational mines (Davies, 1967). Inhaled aerosols of these dimensions can reach all parts of the lung (Davies, 1974). A 6.0 MeV, Po-218 α particle has a range of 47 μm and a 7.69 MeV, Po-214 α particle has a range of 70.8 μm (Lea, 1955) in lung tissue.

In a previous study (Bowden and Baldwin, 1989; Baldwin et al, 1991), the thickness of the bronchial epithelium in humans was measured. Although there were considerable variations in thickness, with progressive thinning towards the periphery, (Table 7, Appendix 1), all epithelial nuclei, including those of the basal cells, were within the range of α particle irradiation, (Table 8, Appendix 1) a factor of some significance to uranium miners.

The present study, utilizing the Ki-67 antibody, demonstrated proliferative activity in basal cells and in columnar cells. Study of diurnal variation was not possible because all specimens were surgically removed in the morning. Table 3A depicts the number of labelled and unlabelled cells/mm epithelium. No significant differences were found between the bronchial generations studied. Typical basal cells constitute the majority of the labelled cells ($\geq$0.97/mm of epithelium) and unlabelled cells ($\geq$ 84/mm of epithelium). There are less than 0.32 labelled atypical cells/mm and less than twenty-one unlabelled atypical basal cells/mm.

Typical and atypical basal cells together represent a proliferating basal cell population of $\geq$ 1.29/mm of epithelium in cross sections of bronchi but there are also proliferating cells in the columnar epithelium ($\geq$ 0.20/mm). The percentages of basal cells which are proliferating are small for all generations (Table 4A) with minimum and maximum figures of 0.82% and 2.807% respectively for typical basal cells and 0.424% and 2.096% for atypical basal cells. Differences between generations were not significant (Table 4B). The percentages of labelled cells in the columnar epithelium are unknown because the unlabelled cells were not enumerated, but they are most likely low considering the great cellularity of the epithelium.

The data from this study show that proliferative activity is low in smaller airways (Generations 7-15); the extent of proliferative activity in the upper bronchial tree is unknown, but there might not be great regional differences in proliferative activity. Animal studies show no differences for rate of entry into mitosis (REM) between trachea and small bronchi in adult mice (Bjork and Harkonen, 1960), but in young mice the REM for trachea was much greater than the REM for small bronchi (Bjork, 1957).

Calculations of the number of labelled cells for each generation (Table 5B), and the certainty that all nuclei are within range of α particles at the mucociliary surface (Bowden and Baldwin, 1989; Baldwin et al, 1991), indicate the cell population at risk.

Detailed enumeration of Ki-67 labelled cells in metaplastic and hyperplastic epithelium was not undertaken. In many focal areas of metaplasia there was no proliferative activity; when there was proliferative activity, numerous labelled cells were distributed throughout the metaplastic epithelium (Figure 10). For example, in a section through a 250 μm length of metaplastic epithelium, four

to five cells thick, there were thirty-six labelled cells, only a few of which were in the basal part of the epithelium. In another area of metaplasia, three to four cells thick, there were twenty-one labelled cells, but only three were in a basal location. Clearly a focus of metaplasia can have a high level of proliferative activity/mm epithelium far exceeding that of normal epithelium (> 2/mm). The large number of proliferating cells mark foci of developing bronchial metaplasia as important targets well within range of the effects of particles at the mucociliary surface (Bowden and Baldwin, 1989; Baldwin et al, 1991).

We have no data on non-smokers. Comparisons between former smokers and long term smokers (Table 6A) reveal significant differences in the number of proliferating basal cells/mm epithelium between the two groups. In former smokers there are more proliferating typical basal cells (P=0.006) and atypical basal cells (P=0.002) /mm epithelium. In generations 12-15 there are more proliferating columnar cells in ex-smokers than smokers (P=0.001). A variety of agents, including tobacco smoke, are known to stimulate proliferative activity in the airways of experimental animals. From a clinical viewpoint, it is generally held that persons who have ceased smoking for several years and have not developed lung cancer, have a similar low risk of developing lung cancer as persons who have never smoked.

The present study which is of a few lungs only, indicates that in smaller airways proliferation by basal cells and by cells in the columnar epithelium, at least in some airway generations, is significantly greater in former smokers than in current smokers. Thus former smokers might be at increased risk to the effects of α particles at the mucociliary surface.

The columnar cells of bronchial epithelium are known to be joined to one another by junctions (Figures 13, 16). Cytoplasmic interdigitations perhaps assist cell attachment (Figure 13). However there are no known mechanisms for the attachment of columnar cells to the basement membrane. The classical interpretation, from light microscopy, is that rectangular columnar cells sit on the basement membrane. However electron microscopy shows that the basal aspect of the columar cell is irregular, some cytoplasmic projections reach the basement membrane (Figure 16), and others terminate on underlying basal cells (Figures 12, 13, 16, 19). Both types of basal cell are tightly attached to the basement membrane (Figures 12, 15) and to one another (Figures 20, 21, 22, 23) by desmosomes. Their close adhesion is exemplified by the way they remain in place when other columnar cells become detached in a sheet as a consequence of mild mechanical force, for example, damage caused by instruments during dissection.

Both types of basal cell provide anchorage for columnar cells. Individually the elongated cell body and attenuated processes of atypical basal cells offer a greater surface (Figure 13, 14, 16)

for attachment than the pyramidal typical basal cells (Figure 12); but collectively the latter, because they are more numerous, provide an extensive surface for epithelial attachment. Between bronchial generations there are no evident differences for atypical basal cells in the extent of cell surface and junctions for columnar cell attachment.

There are no significant differences for the number of basal cells /mm epithelium (Table 3B) or in percentages of the two basal cell types calculated from these figures (Generation 7, 20% atypical basal cells; Generation 13, 25% atypical basal cells). The percentages of basal cell types are similar in larger bronchi (Bowden and Baldwin, 1989).

From investigation of the trachea, a role in epithelial cohesiveness has been proposed for basal cells whose number and surfaces for columnar cell attachment are greater where epithelium is the tallest (Evans and Plopper, 1988; Evans et al, 1989). However the present study shows that the basal cell population/mm epithelium is similar for all generations (Table 3B) and not correlated with differences in epithelial height, which is known to decrease with successive generations of the bronchial tree.

Comparisons of fine structure and filament immunostaining show that neither basal cell types are contractile and any similarities betweem atypical basal cells and myoepithelial cells are superficial only.

It has long been understood that human bronchial epithelium is comprised of ciliated and unciliated columnar cells, mucous cells and basal cells, but it is now known that the nature of the epithelium is more complex.

It is evident that there are two types of basal cell, both are proliferative, the typical basal cell provides the greater proliferating population and is the principal progenitor. Both cell types provide the mechanism for maintaining epithelial attachment to the basement membrane, but the atypical basal cell is more specialized for the role.

Special stains reveal some additional cellular constituents. Some, such as macrophages and lymphocytes, are most likely cells in transit across the epithelium; neuroendocrine cells and dendritic cells are more permanent members within the epithelium. Neuroendocrine cells occur as solitary cells or in groups as neuroepithelial bodies; their proliferative capacity in human bronchial epithelium is unclear, although there are some indications that similar cells proliferate in pulmonary epithelium of rodents (Sorokin et al, 1982; Sarikas et al, 1985; Carabba et al, 1985; Cutz et al, 1985; Monuenga et al, 1991) and human fetal lung (McDougall, 1978). Antigen processing dendritic cells form a network in the basal part of the epithelium, but their

proliferative role in human bronchial epithelium is unknown. From studies of antigen producing dendritic cells in lymphoid tissue, the preponderant notion has been that dendritic cells are end cells incapable of further division (Stingl et al, 1980). However, mitosis of antigen processing cells has been reported in the spleen (Steinman and Cohn, 1974) and epidermis (Hashimoto and Ternowski, 1968; Miyauchi and Hashimoto, 1987; Gschnait and Brenner, 1979; Czernielewski et al, 1985).

Without special stains neither solitary neuroendocrine cells nor dendritic cells can be distinguished with certainty. In the basal layer of human bronchial epithelium where most dividing cells are located, small numbers of solitary neuroendocrine cells and dendritic cells are scattered among elements usually identified as basal cells in routinely stained preparations. However, until the proliferative capacity of neuroendocrine cells and dendritic cells is clarified, the possibility that a small number of the Ki-67 labelled cells in human bronchial epithelium might not be epithelial progenitors cannot be ruled out entirely.

TABLE 1
Ki-67 LABELLED BASAL AND COLUMNAR CELLS AND TOTAL BASAL CELLS

BRONCHIAL GENERATION **	DIAMETER (mm)	n=*	LABELLED CELLS TYPICAL BASAL	LABELLED CELLS ATYPICAL BASAL	LABELLED CELLS COLUMNAR	n=*	TOTAL BASAL CELLS TYPICAL	TOTAL BASAL CELLS ATYPICAL
15	0.40	6	1.00 ± 0.0	0.50 ± 0.22	0.0 ± 0.0	3	84 ± 5	7 ± 2
13	0.62	6	2.33 ± 0.21	0.33 ± 0.21	0.33 ± 0.2	3	255 ± 19	71 ± 3
13	0.66	6	1.00 ± 0.26	0.67 ± 0.21	0.0 ± 0.0	3	110 ± 12	25 ± 5
13	0.66	5	1.80 ± 0.37	1.00 ± 0.0	0.20 ± 0.20	3	141 ± 21	33 ± 2
12	0.72	6	2.67 ± 0.21	1.00 ± 0.0	0.17 ± 0.17	3	104 ± 11	27 ± 2
12	0.76	3	1.66 ± 0.33	0.0 ± 0.0	0.0 ± 0.0	3	82 ± 8	22 ± 5
12	0.76	8	5.37 ± 0.26	1.25 ± 0.16	2.0 ± 0.27	3	380 ± 1	79 ± 5
12	0.79	6	2.66 ± 0.33	0.66 ± 0.21	0.17 ± 0.17	3	101 ± 7	36 ± 2
12	0.80	4	1.25 ± 0.25	0.25 ± 0.25	0.0 ± 0.0	3	109 ± 5	42 ± 1
11	0.97	9	3.88 ± 0.20	0.44 ± 0.18	0.22 ± 0.15	3	103 ± 8	53 ± 1
11	0.98	9	3.11 ± 0.26	1.00 ± 0.17	0.55 ± 0.18	4	84 ± 3	42 ± 5
11	1.03	4	1.75 ± 0.25	1.00 ± 0.41	0.0 ± 0.0	3	143 ± 1	22 ± 2
11	1.14	5	4.20 ± 0.37	0.40 ± 0.24	0.40 ± 0.24	2	161 ± 2	70 ± 6
11	1.15	4	2.50 ± 0.29	0.25 ± 0.25	0.25 ± 0.25	3	92 ± 10	25 ± 2
10	1.28	4	3.00 ± 0.41	1.00 ± 0.0	0.50 ± 0.29	3	155 ± 5	22 ± 1
10	1.34	4	4.25 ± 0.25	1.25 ± 0.25	0.0 ± 0.0	3	351 ± 11	47 ± 10
10	1.38	6	6.83 ± 0.31	0.66 ± 0.21	1.00 ± 0.26	3	296 ± 14	52 ± 5
10	1.44	6	2.00 ± 0.26	0.33 ± 0.21	0.17 ± 0.17	3	173 ± 3	46 ± 3
10	1.46	5	5.00 ± 0.32	0.60 ± 0.24	0.60 ± 0.24	4	300 ± 19	47 ± 5
9	1.54	4	3.25 ± 0.25	0.0 ± 0.0	0.0 ± 0.0	3	329 ± 2	57 ± 1
9	1.78	4	1.50 ± 0.29	0.5 ± 0.29	0.0 ± 0.0	3	230 ± 10	59 ± 1
8	1.86	6	2.00 ± 0.26	0.0 ± 0.0	0.0 ± 0.0	3	230 ± 10	68 ± 13
8	1.90	4	2.25 ± 0.25	1.75 ± 0.25	1.0 ± 0.41	3	244 ± 11	64 ± 8
8	1.91	7	3.71 ± 0.28	0.71 ± 0.18	0.85 ± 0.14	3	190 ± 1	36 ± 1
7	2.13	5	4.68 ± 0.60	0.20 ± 0.20	0.80 ± 0.49	3	465 ± 8	56 ± 6
7	2.37	6	2.17 ± 0.17	0.50 ± 0.22	0.17 ± 0.17	3	86 ± 12	18 ± 2
7	2.49	18	3.06 ± 0.42	0.61 ± 0.18	0.61 ± 0.18	3	226 ± 9	72 ± 2
7	2.58	6	9.83 ± 1.11	1.00 ± 0.26	1.5 ± 0.34	3	250 ± 8	63 ± 6

Numbers represent means ± standard deviation.
* n = number of sections from which data is derived.
** Weibel (1963)

TABLE 2
Ki-67 LABELLED BASAL AND COLUMNAR CELLS AND TOTAL BASAL CELLS PER mm OF EPITHELIUM

BRONCHIAL GENERATION*	DIAMETER (mm)	CIRCUMFERENCE	TOTAL BASAL CELLS TYPICAL	ATYPICAL	TOTAL
15	0.40	1.256	67	6	73
13	0.62	1.947	131	36	167
13	0.66	2.073	53 } 84 ± 41	12 } 21 ± 13	65 } 105 ± 54
13	0.66	2.072	68	16	84
12	0.72	2.261	46	12	58
12	0.76	2.387	34	9	43
12	0.76	2.377	160 } 65 ± 53	33 } 17 ± 9	193 } 82 ± 62
12	0.79	2.481	41	14	55
12	0.80	2.513	43	17	60
11	0.97	3.035	34	17	51
11	0.98	3.078	27	14	41
11	1.03	3.244	44 } 35 ± 9	7 } 13 ± 6	51 } 48 ± 12
11	1.14	3.581	45	20	65
11	1.15	3.612	25	7	32
10	1.28	4.021	38	5	44
10	1.34	4.220	83	11	94
10	1.38	4.335	68 } 59 ± 20	12 } 10 ± 3	80 } 69 ± 22
10	1.44	4.523	38	10	48
10	1.46	4.586	65	10	75
9	1.54	4.838	68	12	80
9	1.78	5.592	41 } 54 ± 19	11 } 11 ± 1	52 } 65 ± 20
8	1.86	5.843	39	12	51
8	1.90	5.969	41 } 37 ± 5	11 } 9 ± 3	52 } 46 ± 8
8	1.91	6.0	32	6	38
7	2.13	6.691	69	8	78
7	2.37	7.456	12	2	14
7	2.49	7.822	29 } 35 ± 24	9 } 7 ± 3	38 } 42 ± 26
7	2.58	8.114	31	8	39

Numbers represent means ± standard error.
*Weibel (1963).
** Greater than mean because of wide variability

(TABLE 2 - continued)

TYPICAL BASAL	ATYPICAL BASAL	TOTAL	COLUMNAR
0.80 1.20 0.49 0.87 } 0.85 ± 0.36	0.40 0.17 0.32 0.48 } 0.32 ± 0.16	1.19 1.37 0.80 1.35 } 1.17 ± 0.32	0 0.17 0 0.10 } 0.09 ± 0.09
1.18 0.70 2.26 1.07 0.50 } 1.14 ± 0.68	0.46 0 0.52 0.27 0.1 } 0.27 ± 0.22	1.62 0.70 2.79 1.34 0.60 } 1.41 ± 0.88	0.07 0 0.84 0.07 0 } 0.20 ± 0.36 **
1.28 1.01 0.54 1.17 0.69 } 0.94 ± 0.32	0.15 0.32 0.31 0.11 0.07 } 0.19 ± 0.12	1.43 1.34 0.85 1.28 0.76 } 1.13 ± 0.30	0.07 0.18 0 0.11 0.07 } 0.09 ± 0.07
0.75 1.01 1.57 0.44 1.09 } 0.97 ± 0.42	0.25 0.30 0.15 0.07 0.13 } 0.18 ± 0.09	0.99 1.30 1.73 0.51 1.22 } 1.15 ± 0.44	0.12 0 0.23 0.04 0.13 } 0.10 ± 0.09
0.67 0.27 } 0.47 ± 0.29	0 0.09 } 0.04 ± 0.06 **	0.67 0.36 } 0.51 ± 0.22	0 0 } 0 ± 0
0.34 0.38 0.62 } 0.45 ± 0.15	0 0.29 0.12 } 0.14 ± 0.15 **	0.34 0.67 0.74 } 0.58 ± 0.21	0 0.17 0.4 } 0.10 ± 0.09
0.69 0.29 0.39 1.21 } 0.64 ± 0.41	0.03 0.07 0.08 0.12 } 0.07 ± 0.04	0.72 0.36 0.44 1.34 } 0.72 ± 0.44	0.12 0.02 0.08 0.18 } 0.10 ± 0.07

LABELLED CELLS

TABLE 3 A
ANALYSIS OF LABELLED CELLS PER mm OF EPITHELIUM

BRONCHIAL GENERATION *	7	8	9	10	11
BRONCHIAL DIAMETER (mm)	2.13 - 2.58	1.86 - 1.91	1.54 - 1.78	1.28 - 1.46	0.15 - 0.97
BASAL CELLS					
TYPICAL	0.64 ± 0.41	0.45 ± 0.15	0.47 ± 0.29	0.97 ± 0.42	0.94 ± 0.32
ATYPICAL	0.07 ± 0.04	0.14 ± 0.15 **	0.04 ± 0.06 **	0.18 ± 0.09	0.19 ± 0.12
TOTAL	0.72 ± 0.44	0.58 ± 0.21	0.51 ± 0.22	1.15 ± 0.44	1.13 ± 0.44
COLUMNAR CELLS	0.10 ± 0.07	0.10 ± 0.09	0 ± 0	0.10 ± 0.09	0.09 ± 0.07

TABLE 3 B
ANALYSIS OF BASAL CELLS PER mm OF EPITHELIUM

BRONCHIAL GENERATION *	7	8	9	10	11
BRONCHIAL DIAMETER (mm)	2.13 - 2.58	1.86 - 1.91	1.56 - 1.78	1.28 - 1.46	0.15 - 0.97
BASAL CELLS					
TYPICAL	35 ± 24	37 ± 5	54 ± 19	59 ± 20	35 ± 9
ATYPICAL	7 ± 3	9 ± 3	11 ± 1	10 ± 3	13 ± 6
TOTAL	42 ± 26	47 ± 8	66 ± 20	68 ± 22	48 ± 12

Numbers represent means ± standard error.
*Weibel (1963).
**Greater than mean because of wide variability

TABLES 3A and 3B - continued

12	13	15	P Values	P(log)
0.72 - 0.80	0.62 - 0.66	0.40		
1.14 ± 0.68	0.85 ± 0.36	0.80	0.40	0.31
0.27 ± 0.22	0.32 ± 0.16	0.40	0.16	0.16
1.41 ± 0.88	1.17 ± 0.32	1.19	0.28	0.18
0.20 ± 0.36	0.09 ± 0.09	0	0.92	0.92

12	13	15	P Values	P(log)
0.72 - 0.80	0.62 - 0.66			
65 ± 53	84 ± 41	67	0.38	0.16
17 ± 9	21 ± 13	6	0.14	0.07
82 ± 62	105 ± 54	73	0.36	0.18

TABLE 4A
LABELLED BASAL CELLS AS A PERCENTAGE OF TOTAL BASAL CELLS

BRONCHIAL* GENERATION	BRONCHIAL DIAMETER (mm)	BASAL CELLS TYPICAL		BASAL CELLS ATYPICAL		BASAL CELLS TOTAL	
15	0.40	1.195		7.143		1.654	
13	0.62	0.915		0.472		0.819	
13	0.66	0.912	1.033 ± 0.21	2.666	2.066 ± 1.40	1.238	1.222 ± 0.40
13	0.66	1.274		3.061		1.609	
12	0.72	2.572		3.750		2.813	
12	0.76	2.041		0		1.608	
12	0.76	1.414	1.963 ± 0.67	1.589	1.561 ± 1.44	1.444	1.860 ± 0.75
12	0.79	2.640		1.869		2.439	
12	0.80	1.147		0.595		0.993	
11	0.97	3.776		0.839		2.778	
11	0.98	3.704		2.395		3.269	
11	1.03	1.221	2.807 ± 1.04	4.545	1.867 ± 1.66	1.663	2.410 ± 0.63
11	1.14	2.609		0.571		1.991	
11	1.15	2.727		0.987		2.350	
10	1.28	1.940		4.545		2.264	
10	1.34	1.212		2.660		1.383	
10	1.38	2.311	1.657 ± 0.49	1.274	2.096 ± 1.54	2.155	1.697 ± 0.51
10	1.44	1.157		0.725		1.065	
10	1.46	1.668		1.277		1.615	
9	1.54	0.988		0		0.841	
9	1.78	0.653	0.820 ± 0.24	0.847	0.424 ± 0.60 **	0.693	0.767 ± 0.10
8	1.86	0.868		0		0.670	
8	1.90	0.922	1.250 ± 0.61	2.720	1.562 ± 1.404	1.297	1.309 ± 0.64
8	1.91	1.958		1.966		1.960	
7	2.13	0.989		0.357		0.921	
7	2.37	2.519		2.727		2.556	
7	2.49	1.52	2.198 ± 1.33	0.849	1.380 ± 1.03	1.230	2.042 ± 1.18
7	2.58	3.933		1.587		3.461	

Numbers represent means ± standard error.
*Weibel (1963).
**Greater than mean because of wide variability

TABLE 4 B
ANALYSIS OF LABELLED BASAL CELLS AS A PERCENTAGE OF TOTAL BASAL CELLS

BRONCHIAL GENERATION *	7	8	9	10	11	12	13	15	P Values
BRONCHIAL DIAMETER (mm)	2.13 - 2.58	1.86 - 1.91	1.54 - 1.78	1.28 - 1.46	0.97 - 1.15	0.72 - 0.80	0.62 - 0.66	0.40	
BASAL CELLS									
TYPICAL	2.198 ± 1.33	1.25 ± 0.61	0.82 ± 0.24	1.657 ± 0.49	2.807 ± 1.04	1.963 ± 0.67	1.033 ± 0.21	1.195	0.06
ATYPICAL	1.38 ± 1.03	1.562 ± 1.404	0.424 ± 0.60	2.096 ± 1.54	1.867 ± 1.66	1.561 ± 1.44	2.066 ± 1.40	7.143	0.06
TOTAL	2.042 ± 1.18	1.309 ± 0.64	0.767 ± 0.10	1.697 ± 0.51	2.41 ± 0.63	1.86 ± 0.75	1.222 ± 0.40	1.654	0.18

Numbers represent means ± standard error.
*Weibel (1963).

TABLE 5 A
Ki-67 LABELLED CELLS PER mm LENGTH OF BRONCHI BY GENERATIONS *

BRONCHIAL GENERATION	7	8	9	10	11	12	13	15
BASAL CELLS								
TYPICAL	80	56.25	58.75	121.25	117.50	142.50	106.25	100
ATYPICAL	8.75	17.50	5	22.50	23.75	33.75	40	50
TOTAL	90	72.50	63.75	143.75	141.25	176.25	146.25	148.75
COLUMNAR CELLS	12.5	12.50	0	12.50	11.25	25	11.25	0

TABLE 5 B
Ki-67 LABELLED CELLS IN EACH BRONCHIAL GENERATION *

BRONCHIAL GENERATION	7	8	9	10	11	12	13	15
LENGTH (mm)	7.6	6.4	5.4	4.6	3.9	3.3	2.7	2.0
BASAL CELLS								
TYPICAL	608	360	317.25	557.75	458.25	470.25	286.87	200
ATYPICAL	66.5	112	27	103.5	92.62	111.37	108	100
COLUMNAR CELLS	95	80	0	57.5	43.87	82.5	30.37	0

* Calculated figures.

TABLE 6A
COMPARISONS BETWEEN SMOKERS AND EX-SMOKERS

Ki-67 LABELLED CELLS
PER mm EPITHELIUM

BRONCHIAL GENERATION *	7 - 9		10 - 11		12 - 15	
	Ex-smoker	Smoker	Ex-smoker	Smoker	Ex-Smoker	Smoker
BASAL CELLS						
TYPICAL	0.92 ± 0.30	0.43 ± 0.07	1.08 ± 0.14	0.79 ± 0.21	1.56 ± 0.70	0.85 ± 0.12
ATYPICAL	0.12 ± 0.00	0.08 ± 0.04	0.23 ± 0.04	0.14 ± 0.05	0.50 ± 0.02	0.24 ± 0.06
TOTAL	1.04 ± 0.30	0.51 ± 0.06	1.31 ± 0.12	0.93 ± 0.22	2.07 ± 0.72	1.09 ± 0.15
COLUMNAR	0.16 ± 0.02	0.06 ± 0.03	0.10 ± 0.04	0.09 ± 0.03	0.47 ± 0.37	0.04 ± 0.02

Numbers represent means ± standard error.
*Weibel (1963).

SIGNIFICANT P VALUES

	Ex-Smokers vs Smokers			Generations 7-9 vs Generations 12-15	
Ki-67 LABELLED CELLS PER mm EPITHELIUM	All Generations	Generations 7-9	Generations 12-15	Ex-Smokers	Ex-smokers and Smokers
BASAL CELLS					
TYPICAL	0.006				0.054
ATYPICAL	0.002				0.014
TOTAL	0.005				0.01
COLUMNAR			0.001		

TABLE 6B
COMPARISONS BETWEEN SMOKERS AND EX-SMOKERS

BASAL CELLS PER
mm EPITHELIUM

BRONCHIAL GENERATION*	7 - 9		10 - 11		12 - 15	
	Ex-Smoker	Smoker	Ex-Smoker	Smoker	Ex-Smoker	Smoker
TYPICAL	31.2 ± 0.4	42.8 ± 7.8	53.7 ± 8.9	40.6 ± 2.2	114.0 ± 45.8	59.2 ± 12.6
ATYPICAL	6.9 ± 0.8	9.3 ± 1.2	16.9 ± 1.4	11.7 ± 4.1	24.00± 8.7	15.1 ± 3.8
TOTAL	38.1 ± 0.4	52.0 ± 8.6	65.6 ± 8.5	52.3 ± 6.2	138 ± 54.5	74.4 ± 15.8

Numbers represent means ± standard error.
*Weibel (1963).

SIGNIFICANT P VALUES

BASAL CELLS PER mm EPITHELIUM	Ex-Smokers vs Smokers			Generations 7-9 vs Generations 12-15	
	All Generations	Generations 7-9	Generations 12-15	Ex-Smokers	Ex-smokers and Smokers
BASAL CELLS					
TYPICAL				0.007	
ATYPICAL					0.02
TOTAL				0.006	

TABLE 6C
COMPARISONS BETWEEN SMOKERS AND EX-SMOKERS

Ki-67 LABELLED BASAL CELLS
AS A PERCENTAGE OF TOTAL
BASAL CELLS PER mm EPITHELIUM

BRONCHIAL GENERATION*	7 - 9		10 - 11		12 - 15	
	Ex-Smoker	Smoker	Ex-Smoker	Smoker	Ex-Smoker	Smoker
TYPICAL	2.95 ± 0.99	1.18 ± 0.24	2.32 ± 0.48	1.90 ± 0.42	1.34 ± 0.07	1.63 ± 0.29
ATYPICAL	1.78 ± 0.19	1.07 ± 0.45	2.16 ± 0.56	1.95 ± 1.3	2.32 ± 0.74	2.36 ± 0.94
TOTAL	2.71 ± 0.75	1.17 ± 0.25	2.14 ± 0.30	1.77 ± 0.36	1.53 ± 0.08	1.65 ± 0.28

Numbers represent means ± standard error.
*Weibel (1963).

SIGNIFICANT P VALUES

Ki-67 LABELLED BASAL CELLS AS A PERCENTAGE OF TOTAL BASAL CELLS PER mm EPITHELIUM	Ex-Smokers vs Smokers			Generations 7-9 vs Generations 12-15	
	All Generations	Generations 7-9	Generations 12-15	Ex-Smokers	Ex-smokers and Smokers
BASAL CELLS					
TYPICAL		0.02			
ATYPICAL					
TOTAL		0.02			

TABLE 7 *
EPITHELIAL MEASUREMENTS (μm)

AIRWAY GENERATION	1	2	3	4	5 - 7	7 - 16	P Values
AIRWAY DIAMETER	≥ 9.02	7.01 - 9	5.51 - 7	4.51 - 5.5	2.01 - 4.5	0.26 - 2	
CELL TYPE							
BASAL TYPICAL							
CILIA	6.85 ± 0.19	6.44 ± 0.45	6.18 ± 0.26	6.40 ± 0.17	5.89 ± 0.27	5.69 ± 0.15	0.0685
APEX OF CELL TO NUCLEUS	26.65 ± 2.36	25.83 ± 3.96	24.08 ± 2.22	22.02 ± 1.29	24.59 ± 1.76	17.46 ± 0.93	0.0033
NUCLEUS	4.71 ± 0.28	4.87 ± 0.44	4.54 ± 0.21	4.58 ± 0.20	4.69 ± 0.20	4.26 ± 0.18	0.5415
APEX TO EPITHELIAL BASEMENT MEMBRANE	33.35 ± 2.73	32.62 ± 4.59	30.28 ± 2.45	27.91 ± 1.55	31.03 ± 2.00	23.15 ± 1.13	0.0052
BASAL ATYPICAL							
CILIA	5.99 ± 0.19	5.89 ± 0.63	6.17 ± 0.45	5.80 ± 0.24	5.79 ± 0.15	5.77 ± 0.19	0.9042
APEX OF CELL TO NUCLEUS	23.34 ± 2.40	21.33 ± 5.07	17.19 ± 1.36	20.11 ± 1.84	18.15 ± 1.08	15.98 ± 1.19	0.0686
NUCLEUS	3.11 ± 0.15	2.96 ± 0.36	2.81 ± 0.15	4.23 ± 1.56	2.83 ± 0.05	2.79 ± 0.09	0.6681
APEX TO EPITHELIAL BASEMENT MEMBRANE	27.72 ± 2.61	25.12 ± 5.19	20.90 ± 1.43	21.96 ± 1.22	21.90 ± 2.09	19.59 ± 1.27	0.0396

Numbers represent means ± standard error.
Measurements for cilia and apex of cell to basal cell nucleus are for cells overlying the basal cell.
Measurements apex to epithelial basement membrane are for epithelial cell adjacent to basal cell.
* Baldwin et al 1991

REFERENCES

Auerbach, O. Natural History of Carcinoma of the Lung. Pulmonary Diseases and Disorders. Ed. A.P. Fishman., McGraw-Hill; New York. 1388; 1980.

Ayers, M.M., Jeffery, P.K. Cell division and differentiation in bronchial epithelium. In: Cellular biology of the lung. eds. G. Bonsignore & I. Cumming, Plenum; New York. 33-59; 1982.

Ayers, M.W., Jeffery, P.K. Proliferation and differentiation in mammalian airway epithelium. Eur. Respir. J. 1: 58-80; 1988.

Baldwin, F., Hovey, A., McEwen, T., O'Connor, R., Unruh, H., Bowden, D.H. Surface to nuclear distances in human bronchial epithelium: relationships to penetration by Rn daughters. Health Physics. 60:(2): 155-162; 1991.

Becci, P.J., McDowell, E.M., Trump, B.F. The Respiratory Epithelium. II Hamster Trachea, Bronchus and Bronchioles. Natl. Cancer Inst. 61: 551-561; 1978.

Bertanlanffy, F.D., Leblond, C.P. The continuous renewal of two types of alveolar cells in the lung of the rat. Anat. Dec. 115: 515; 1953.

Bindreiter, M., Shuppler, J., Stockinger L. Zellproliferation and Differenzierung im Tracheal Epithel Der Ratte. Exp. Cell Res. 50: 377; 1968.

Bjork, H. Mitotic rate colchicine sensitivity of the epithelium of oesophagus, trachea and bronchi of the white mouse. Ann. Med. Exptl. Fenn. 35: 223-232; 1957.

Bjork, H., Harkonen, W. Mitotic activity in the epithelium of the oesophagus, trachea and small bronchi of two and three month old mice. Ann. Med. Exptl. Fenn. 38: 288-292; 1960.

Boren, H.G., Paradise, L.J. Cytokinetics of the Lung in Pathogenesis and Therapy of Lung Cancer. Ed. C.C. Harris, Marcel Dekker; New York. 369-418; 1978.

Bowden, D.H., Baldwin, F. Measurement of the thickness of the bronchial epithelium. A research report to the atomic Energy Control Board of Canada; 1989.

Bowden, D.H. Cell turnover in the lung. Am. Rev. Respir. Dis. 128: 546-548; 1983.

Braun, N., Papadopoulos, T., Muller-Hermelink H.K. Cell proliferation dependent distribution of the proliferative-associated Ki-67 antigen in human embryonic lung cells. Virchows Arch. (B.) Cell Pathol. 56: 25-33; 1988.

Breuer, R., Zajicek, G., Christensen, T.G., Lucey, E.C. Snider, G.L. Cell Kinetics of normal adult hamster bronchial epithelium in the steady state. American Journal of Respiratory Cell and Molecular Biology 2: 51-58; 1990.

Breuer, R., Zajicek, G., Christensen, T.G., Lucey, E.C. Snider, G.L. Cell Kinetics of normal adult hamster bronchial epithelium in the steady state. American Journal of Respiratory Cell and Molecular Biology 2: 51-58; 1990.

Burger, P.C., Shibata, T., Kleihues, P. The use of the monoclonal antibody Ki-67 in the identification of proliferating cells. Am. J. Surg. Path. 10: 611-617; 1986.

Carabba, V.H., Sorokin, S.P., Hoyt, R.F. Development of neuroepithelial bodies in intact and cultured lungs of fetal rats. Am. J. Anat. 173: 1-27; 1985.

Chamberlain A.C., Dyson, E.D. The doses to the trachea and bronchi from the decay products of radon and thoron. Br. J. Radiol. 29: 317-327; 1956.

Committee on the Biological Effects of Ionizing Radiation (BEIR III). Health Risks of radon and other internally deposited alpha-emitters. National Academy Press, Washington, D.C.: 1980.

Committee on the Biological Effects of Ionizing Radiation (BEIR IV). Health risks of radon and other internally deposited alpha-emitters. National Academy Press, Washington, D.C.: 1988.

Cordell, J.L., Felini, B., Erber, W.N. Immunoenzymatic labelling of monocloncal antibodies using immune complexes of alkaline phosphatase and monoclonal anti-alkaline phosphatase (APAAP) complexes. J. Histochem. Cytochem. 32: 219-229; 1984.

Cutz, E., Yeger, H., Wong, V., Bienkowski, E., Chan, W. In vitro characteristics of pulmonary neuroendocrine cells isolated from rabbit fetal lung. I Effects of culture media and nerve growth factor. Lab. Invest. 55: 672-683; 1985.

Czernielewski, J., Vaigot, P., Prunieras, M. Epidermal Langerhans cells - a cycling cell population. J. Invest. Dermatol. 84: 424-426; 1985.

Das, E.W., Jain, M., Thurlbeck, W.M. Diurnal variation of deoxyribonucleic acid synthesis in murine alveolar wall cells and airway epithelial cells. Am. J. Respir. Dis. 119: 81-85; 1979.

Davies, C.N. Aerosol sampling related to inhalation. In: Assessment of airborne radioactivity. Symposium on instruments and techniques for the assessment of airborne radioactivity in nuclear operations. Vienna: International Atomic Energy Agency: 3-22; 1967.

Davies, C.N. Deposition of inhaled particles in man. Chem. Ind. (London) 11: 441-444; 1974.

Donnelly, G.M., Haack, D.G., Heird, C.S. Tracheal Epithelium: Cell Kinetics and Differentiation in Normal Rat Rissue. Cell Tissue Kinet. 15: 1190-130; 1982.

Evans, M.J. Shami, S.G., Cabral-Anderson, L.J., Dekker, N.P. Role of Non-Ciliated Cells in Renewal of the Bronchial Epithelium of Rats exposed to No_2. Am. J. Pathol. 123: 126-133, 1986.

Evans, M.J., Plopper, C.G. The role of basal cells in adhesion of columnar epithelium to airway basement membrane. Am. Rev. Respir. Dis. 138: 481-481; 1988.

Evans, M.J., Cox, R.A., Shami, S.G., Wilson, B., Plopper, C.G. The role of basal cells in attachment of columnar cells to the basal lamina of the trachea. Am. J. Respir. Cell Mol. Biol. 1: 463-469; 1989.

Evans N. Mitotic figures in malignant tumors as effected by time before fixation of tissues. Arch. Pathol. 1: 894-898; 1926.

Galand, P., Degraef L.C. Cyclin/PCWA immunostaining as an alternative to tritiated thynidine pulse labelling for marking S-phase cells in paraffin reactions from animal and human tissues. Cell tissue Kinet. 2: 383-392; 1989.

Gastineau, R.M., Walsh, P.J. Underwood, N. Thickness of bronchial epithelium with relation to exposure to radon. Health Phys. 23: 857-860; 1972.

Gatter, N.C., Dunnill, M.S., Gerdes, J., Stein, H., Mason, D.Y. New approach to assessing lung tumors in man. Clin. Pathol. 39: 590-593; 1986.

Gerdes, J., Schwab, U., Lemke, H., Stein, H. Production of a mouse monoclonal antibody reactive with a human antigen associated with cell proliferation. Int. J. Cancer 31: 13-20; 1983.

Gerdes, J., Lemke, H., Baische, H., Wacker, H.H., Schwab, U., Stein, H. Cell cycle analysis of a cell proliferation associated human nuclear antigen defined by the monoclonal antibody Ki-67. J. Immunol. 133L 1710-1715; 1984.

Graem W., Helweg-Larsen, R. Mitotic activity and delay in fixation of human tissue. Acta Path. Microbiol. Scand. A. 87: 375-378; 1979.

Gschnait, F., Brenner, W. Kinetics of epidermal Langerhans cells. J. Invest. Dermatol. 73:566-569; 1979.

Hall, P.A., Stearn P.M., Butler, M.G., d'Ardenne A.J. Acetone/periodate-lysine-paraformaldehyde (PLP) fixation and improved morphology of cryostat sections for immunohistochemistry. Histopathology 1: 93-102; 1987.

Hall, P.A., Levison, D.A. Assessment of cell proliferation in histological material. J. Clin. Pathol. 43: 184-132; 1990.

Hashimoto, K., Tarnowski, W.M. Some new aspects of the Langerhans cell. Arch. Derm. 97: 450-464; 1968.

Hsu, S.- M., Raine, L., Fanger, H. Use of avidin-biotin-peroxidase complex (ABC) in immunoperoxidase techniques. J. Histochem. Cytochem. 29: 577-580;I981.

Hsu, S.- M., Raine, L., The use of avidin-biotin-peroxidase complex (ABC) in diagnostic and research pathology. In: Advances in Immunohistochemistry. ed. R.A. Delillis, Masson; New York: 33.

Inayama, Y., Hook, G.E., Brody, A.R., Cameron, G.S., Jetten, A.M., Gilmore, L.B., Gray, T., & Nettesheim, P. The differentiation potential of tracheal basal cells. Laboratory Investigation 58: 706-717; 1988.

International Committee on Radiological Protection. Lung cancer risk from indoor exposures to radon daughters. Pergamon, Oxford Press: Ann. ICRP 7: 1: 1987.

Jeffery, P.K., Reid, L.M. The ultrastructure of normal large bronchi. Bronches 23: 368-380; 1973.

Jeffery, P.K., Reid, L. New observations of rat airway epithelium: a quantitative electron microscopic study. J. Anat. 12: 295-320; 1975.

Jeffery, P.K., Reid, L.M. Ultrastructure of airway epithelium and submucosal gland during development. In: Development of the Lung. Ed. W.A. Hodson, Marcel Dekker; New York. 87-134, 1977.

Kamel, O.W., Franklin, W.A., Ringus, J.C., Meyer, J.S. Thymidine labelling index and NI-67 growth fraction in lesion of the breast. Am. J. Pathol. 134: 107-118; 1989.

Keenan, K.P., Combs, J.W., McDowell, E.M. Regeneration of hamster tracheal epithelium after mechanical injury. I. Focal lesions: quantitative morphological study of cell proliferation. Virchows Archiv (Cell Pathology) 41: 193-214; 1982a.

Keenan, K.P., Combs, J.W., McDowell, E.M. Regeneration of hamster tracheal epithelium after mechanical injury. II. Multifocal lesions: stathmokinetic and autoradiographic studies of cell proliferation. Virchows Archiv (Cell Pathology) 41: 215-229; 1982b.

Kmoch, N., Hoffman, N., Spielhoff R., Mohr, U. Circadian periodicity of ^{3}H-thymidine uptake in the Hamster respiratory tract. Int. J. Chronobiol. 3: 63-66; 1975.

Koburg, E. Autoradiographische Untursuchungen zur Zellneubildungstrate au den Epithelien des oberen Respirationsund Verdaungstraktes. Arch. Ohren-Nasen-Kehlkoptheikunde. 180: 616-621; 1962.

Lane, B.P., Gordon R. Regeneration of rat tracheal epithelium after mechanical injury. I. The relationship between mitotic activity and cellular differentiation. Proc. Soc. Exp. Biol. Med. 145: 1139-1144; 1974.

Lea, D.E.A. Action of radiation on living cells. 2nd. ed. Cambridge University Press, Cambridge. MA. 1955.

Lloyd, R.V., Wilson, B.S., Varani, J., Gaur, P.K., Moline, S., Mahari, J.G. Immunocytochemical characterization of a monoclonal antibody that recognizes mitosing cells. Am. J. Pathol. 121: 275-283; 1985.

McDougall, J., Endocrine-like cells in the terminal bronchioles and saccules of human fetal lung: An ultrastructural study. Thorax 33: 43-53; 1978.

McDowell, E.M., Newkirk, C., Coleman, B. Development of Hamster Tracheal Epithelium. II. Cell Proliferation in the Fetus. Anat. Rec. 213: 448-456; 1985.

McDowell, E.M. Combs, J.W. Newkirk, C. A quantitative light and electron microscopic study of hamster tracheal epithelium with special attention to so-called intermediate cells. Exp. Lung Res. 4:205-226; 1983.

McDowell, E.M., Beals, T.F. The bronchial airways in Biopsy Pathology of the Bronchi. Chapman and Hall; London. 49-76; 1986.

Messier, B., LeBlond, C.P. Cell proliferation and migration as revealed by autoradiography after injection of thymidine-H^3 into male rats and mice. J. Anat. 106: 247-285; 1960.

Miyauchi, S., Hashimoto, K. Epidermal Langerhans cells undergo mitosis during the early recovery phase after ultraviolet-B irradiation. J. Invest, Dermatol. 88: 703-709, 1987.

Monuenga, L.M., Springall, D.R., Gaer, J., Winter, R., Lan Zhao, MacBride, J.T., Barer, G., Polak, J.M. Proliferation of rat lung endocrine cells in hypoxia and normoxia. J. Pathol. (in press) 1991.

Plopper, C.G., Alley, J.L., Weir, A.J. Differentiation of tracheal epithelium during fetal lung maturation in the Rhesus monkey Macaca mulatta. Am. J. Anat. 175:59-71:1986.

Raymond, W.A., Leong, A.S., Bolt, J.W., Millos, J., Jose, J.S. Growth fractions in human prostatic carcinoma determined by Ki-67 immunostaining. J. Pathol. 156: 161-167; 1988.

Romanova, L.N. Diurnal periodicity of mitotic cell division in the interalveolar septa of the rat lungs. Bull. Exp. Biol. Med. 61: 88-31; 1966.

Sarikas, S.N., Hoyt, R.F., Sorokin, S.P. Ontogeny of small granule APUD cells in hamster lung: A morphological study. Anat. Rec. 213: 396-409; 1985.

Sasaki, M., Murakami, T., Kawasaki, M., Takahashi M. The cell cycle associated change of the Ki-67 reactive nuclear antigen expression. J. Cell Physiol. 133: 579-584; 1987.

Schutte, B., Reynders, M.M.J., Bosman, F.T., Blijham, G.H. Studies with Anti-Bromodeoxyuridine Antibodies: II. Simultaneous Immunocytochemical Detection of Antigen Expression and DNA Synthesis by in Vivo Labeling of Mouse Intestinal Mucosa. The J. Histochem. Cytochem. 35: 371-374; 1987a.

Schutte, B., Reynders, M.M.J., Bosman, F.T., Blijham, G.H. Effect of Tissue Fixation on Anti-bromodeoxyuridine Immunohistochemistry. J. Histochem. Cytochem. 35: 1343-1345; 1987b.

Sevc, J., Kunz, E., Tomasek, L. Placek, V. Horacek, J. Cancer in man after exposure to Rn daughters. Health Phys. 54: 27-46, 1988.

Shepherd N.A., Richman, P.I., England J. Ki-67 derived proliferative activity in colorectal adenocarcinoma with prognostic correlations. J. Path. 155: 213-219; 1988.

Shorter, R.G., Titus, J.L., Divertie, M.B. Cytodynamics in the respiratory tract of the rat. Thorax. 21: 32-35; 1966.

Sokolova, T.N. Properties of the day-night rhythm of mitotic activity of cells from intra-alveolar cells from lungs of growing rats. Bull. Exp. Biol. Med. 81: 226-228; 1975.

Sorokin, S.P., Hoyt, R.F., Grant, M.M. Development of neuroepithelial bodies in fetal rabbit lungs. I. Appearance and functional maturation as demonstrated by high-resolution light microscopy and formaldehyde-induced fluorescence. Exp. Lung Res. 3: 237-259; 1982.

Spencer, H., Anatomy of the Lung. Pathology of the Lung. Pergamon Press; Oxford. 4th Edition, 17; 1985.

Start, R.D., Flynn, M.S., Rogers, U., Smith, J.H.F. Delayed fixation significantly decreases observed mitotic figures in breast carcinoma. J. Pathol.; 1991 (in press).

Steinman, R.M., Cohn, Z.A. Identification of a novel cell type in peripheral lymphoid organs of mice. II Functional properties in vitro. J. Exp. Med. 138: 380-387; 1974.

Stingl, G., Tamaki, K., Katz, S.I. Origin and function of epidermal Langerhans cells. Immunol. Rev. 53: 149-174; 1980.

Verheijen, R., Kuijpers, H.J.H., Schlingemann, R.O., Boehmer, A.L.M., van Driel, R., Brakenhoff, G.J., Rahmaekers F.C.S. Ki-67 detects a nuclear matrix-associated proliferation related antigen. I. Intracellular localization during interphase. J. Cell Sci. 92: 123-130; 1989a.

Verheijen, R., Kuijpers, H.J.H., van Driel, R., Beck, J.L.M., van Dierendonck, J.H., Brakenhoff, G.J., Ramaekers, F.C.S. Ki-67 detects a nuclear matrix-associated proliferation related antigen II Localization in mitotic cells and associated with chromosomes. J. Cell Sci. 92: 531-540; 1989b.

Walker, R.A., Camplejohn R.S. DNA flow cytometry of human breast carcinomas and its relationship to transferring and epidermal growth factor receptor. J. Pathol. 150: 37-49; 1986.

Waseem, N.H., Lane, D.P. Monoclonal antibody analysis of the proliferating cell nuclear antigen (PCNA). Structural conservation and the detection of a nuclear form. J. Cell Sci. 96: 121-129; 1990.

Weibel, E.R. Morphometry of the human lung. Academic Press; New York: 1963.

ACKNOWLEDGEMENTS

Grateful thanks to Terri Haddon, Dana Naskar, and Laura Siemens for manuscript and table preparation.

Health Physics Vol. 60, No. 2 (February), pp. 155–162, 1991
Printed in the U.S.A.

0017-9078/91 $3.00 + .00
© 1991 Health Physics Society
Pergamon Press plc

● *Paper*

SURFACE TO NUCLEAR DISTANCES IN HUMAN BRONCHIAL EPITHELIUM: RELATIONSHIPS TO PENETRATION BY Rn DAUGHTERS

F. Baldwin, A. Hovey, T. McEwen, R. O'Connor, H. Unruh* and D. H. Bowden
Departments of Pathology and Surgery,* University of Manitoba, Winnipeg, Canada

Abstract—**Lung cancer in U miners is thought to be related to the inhalation of particulate Rn daughters. Since the depth of penetration by α particles is short, the thickness of the epithelium lining the bronchial tree may be a critical factor in the development of cancers at specific sites in the lung. The objectives of the study were to measure the thickness of the epithelium at all levels of the human bronchial tree, to determine the distances of epithelial nuclei from the mucociliary surface, and to compare these parameters in smokers and nonsmokers. Twenty-nine surgically removed specimens were examined; 26 were from smokers. No significant differences were found between smokers and nonsmokers, allowing us to treat the 29 cases as a homogeneous group. With progressive divisions of the bronchi, the epithelium decreases in thickness, and distances of nuclei from the surface are also less in the peripheral bronchi. Allowing for artefacts of tissue preparation, the mean distance from the mucociliary surface to the underlying nuclei varies between 17 and 38 μm.**

INTRODUCTION

LUNG cancer is common in U miners, and an unusually high proportion of highly malignant small cell carcinoma has been reported in North America (Saccamano et al. 1971), Czechoslovakia (Horacek et al. 1977), and South Africa (Webster 1969). The unusually high proportion of small cell carcinoma originally observed in the early stages of epidemiologic follow-up of Colorado Plateau U miners declined with later follow-up of the cohort (BEIR IV 1988). In common with other occupationally related cancers of the lung, smoking is thought to exert a greater than additive effect (BEIR III 1980; Sevc et al. 1988), and there might be a multiplicative interaction between the effects of inhaled radioactive materials and cigarette smoking (ICRP 1987; BEIR IV 1988).

Carcinogenesis in U miners is related to U decay with the production of Rn daughters that attach to molecules of water vapor or dust particles as "cluster ions" (Chamberlain and Dyson 1956). Davies (1967) calculated the mean radioactive diameter of these cluster as 0.25 μm in nonoperational mines and 0.4 μm in operational mines. When inhaled, aerosols of these dimensions can reach all parts of the lung (Davies 1974).

Since the depth of tissue penetration by α particles is short and the predominant population of dividing cells is in the basal layer, the thickness of the epithelial lining at various levels of the bronchial tree may be a critical factor in the initiation of neoplasia at specific sites in the lung. The cells of origin of lung cancer are controversial: some favor the basal cells, others favor secretory cells. The objectives of the study were to measure the thickness of the epithelium at all levels of the human bronchial tree, to determine the distances of the nuclei of basal and other bronchial epithelial cells from the mucociliary surface, and to compare these parameters in groups of smokers and nonsmokers.

(*Manuscript received* 20 *November* 1989; *revised manuscript received* 7 *June* 1990, *accepted* 9 *July* 1990)

MATERIALS AND METHODS

The material examined was obtained from 29 patients undergoing lobectomy or pneumonectomy for the following conditions: primary carcinoma of the lung, 24; metastatic carcinoma, three; hamartoma, one; and nonspecific inflammatory change, one. There were 26 smokers and three nonsmokers. Smoking history, age, and sex are provided in Table 1.

Tissue preparation

Each bronchus of the freshly excised specimen was cannulated and perfused with 10% phosphate buffered formalin, pH 7.0, delivered at a constant pressure of 2.4515 kPa (25 cm of water) for 36 h (Weiss and Tweedale 1966). The fixed specimen was washed in water and, using a rotary meat slicer, 0.5 cm slices were cut to obtain the maximum number of airways in cross section. Portions of tissue were taken for diagnosis and, from the remainder,

Table 1. Smoking history of subjects studied.

Smoking history/ pack years	Age	Sex	
		Male	Female
<25			
4	54	•	
13	70		•
15	61	•	
20	50	•	
23	56		•
≥25			
25	61		•
29	58		•
30	62		•
36	50		•
37	50		•
37	57	•	
40	76		•
47	63	•	
≥50			
50	60		•
50	73	•	
54	67	•	
55	46	•	
60	49	•	
60	62	•	
60	70	•	
68	77	•	
74	67	•	
74	71	•	
94	62	•	
≥100			
100	60	•	
150	64	•	
Nonsmokers	31	•	
	39	•	
	65	•	

blocks containing airways in cross-section were selected for embedding.

The blocks were transferred without washing to glycol methacrylate infiltration medium for two changes of 2 h each, followed by a third infiltration of 16 h and exposure to a vacuum to remove air bubbles. The tissue was then placed in embedding medium on ice and shaken for 30 min, after which it was transferred to embedding medium in a mold and allowed to polymerize at room temperature in a humidity-free environment. The specimens were left in the molds until the sections were to be cut. Blocks were oriented in the microtome so that bronchi were cut in transverse section. Sections were cut at 1.5 μm, dried on a hot plate for 15 min, and stained with toluidine blue-basic fuchsin.

Measurement of bronchi

A stained section of bronchus was projected onto a sheet of paper, the image of the lumen was traced in ink, and the magnification recorded. The diameter of bronchi was computed from the circumferential measurement of the lumen using a MOP-Videoplan image analysis system and standard d-circle measuring programme.*

Measurements of bronchial epithelium

A Quantimet Q-10 image analysis system† was used to make measurements of typical bronchial epithelium (Fig. 1). They were grouped according to bronchial diameters and generations as described by Weibel (1963) (Fig. 2). The number of bronchi and cells measured in each bronchial generation are given in Table 2. Areas of epithelial metaplasia and hyperplasia were also measured.

Statistical methods

Case means and standard errors, by generation and cell type, were computed on the Quantimet Q-10 instrument using standard statistical methods. One-way analysis of variance and modified *t*-tests were performed on an Amdahl-4700 computer, using a Bio-Medical Data Package, Version 5.2.‡

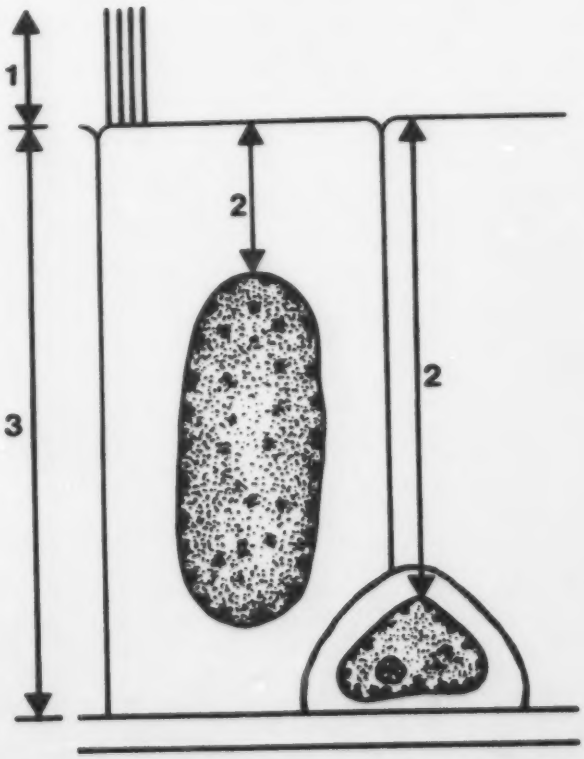

Fig. 1. Bronchial epithelial measurements: 1, cilia; 2, cell surface to nucleus; 3, cell surface to basement membrane.

* Kontron Bildanalyse GMBH, Breslauer Strasse 2, D-8057 Eching, Munich, West Germany.

† Cambridge Instruments Ltd, Rustat Road, Cambridge, England.

‡ BMDP Statistical Software, Inc., 1440 Sepulveda Boulevard, Los Angeles, CA.

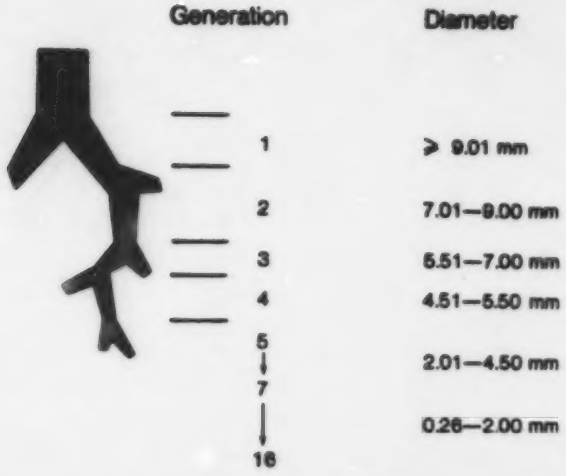

Fig. 2. Bronchial diameters related to bronchial generations (after Weibel 1963).

Artefacts of tissue preparation

The amount of shrinkage or expansion occurring during preparation of the microscopic slides was determined as follows. Slices of lung 1 cm thick (n = 20) were photographed with an accompanying metric scale. Sequential photographs were taken after fixation, embedding, and sectioning (n = 60). Projected images of these photographs were analyzed using a MOP-Videoplan image analysis system; the area of each was compared and expressed as a percentage of the original fresh tissue.

RESULTS

Epithelial morphology

The virtual elimination of preparative artefacts ensured optimal conditions for examination and measurement of the bronchial epithelium. The morphology was remarkably uniform in all of the cases examined (Figs. 3a and b) and, as expected, focal areas of hyperplasia and metaplasia were observed. Two morphologic types of basal cell were identified: the typical small pyramidal cell and a larger elongated cell distributed circumferentially (Figs. 4a and b).

Epithelial measurements

Measurements of epithelial cells were made in 26 smokers and three nonsmokers and the figures submitted to an analysis of variance. There were no significant differences in epithelial thickness when nonsmokers and smokers with different pack-year histories were compared, for example in bronchial generations 4 and 5–7 (Table 3). Since no significant difference was found between the groups analyzed, the 29 cases were considered to represent a homogeneous group and the numbers depicted in subsequent tables are derived from measurements made on smokers and nonsmokers, a total of 29 cases.

Analysis of cell type and bronchial generation

With progressive divisions of the bronchi, the epithelium decreases in thickness (Table 4); for example, the total thickness of ciliated cells, including cilia, in generation 1 is 37.69 ± 2.40 μm and in generations 7–16 the value has decreased to 26.52 ± 1.44 μm ($p = 0.0010$).[1] The critical measurement, cell surface to nucleus for smokers and nonsmokers combined, is provided in Table 5 and Fig. 5. Cell surface to nucleus measurements for smokers and nonsmokers are shown in Figs. 6 and 7, respectively.

Ciliated cells. Cilia tend to be longer in generation 1, 6.52 μm, than in generations 7–16, 5.58 μm (Table 4) ($p = 0.0005$). The mean distance from the cellular surface to the nucleus in generation 1 is 12.86 μm, almost twice the measurement recorded for generations 7–16, 6.53 μm ($p = 0.0010$) (Table 5).

Nonciliated cells and goblet cells. The distances between the surfaces of these cells and their nuclei do not vary significantly throughout the bronchial tree (Table 5).

Typical basal cells. In generation 1, the nucleus of the basal cell is 26.65 μm from the surface, whereas in generations 7–16, the distance is only 17.46 μm ($p = 0.0019$) (Table 5). There are significant differences too between generation 2 and generations 7–16 ($p = 0.0172$), generation 3 and generations 7–16 ($p = 0.0090$), and generations 5–7 and generations 7–16 ($p = 0.0005$).

Atypical basal cells. The distances between the nuclei of these cells and the surface of the overlying cells (Table 5) are significantly different between generations 1 and 3 ($p = 0.0487$), generation 1 and generations 5–7 ($p = 0.0464$), generation 1 and generations 7–16 (p

[1] All p values in parentheses are from analysis of variance.

Table 2. Numbers of bronchi and cells measured.

Bronchial diameter (mm)	>9.01	7.01–9	5.51–7	4.51–5.50	2.01–4.50	0.26–2
Generation[a]	1	2	3	4	5–7	7–16
Bronchi measured	31	9	39	70	207	88
Cells measured	1393	392	1347	2487	6532	2250
Average/bronchus	44.93	43.55	34.53	35.52	31.55	25.56

[a] Weibel (1963).

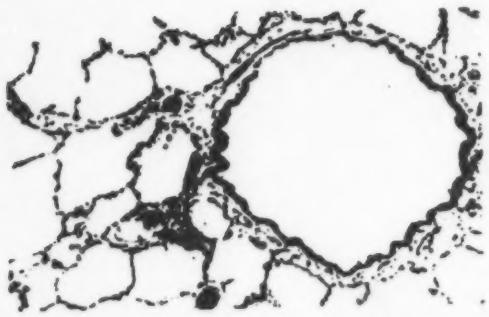

Fig. 3a. Bronchus and alveoli. Toluidine blue–basic fuchsin.

= 0.0061), and generation 4 and generations 7–16 (p = 0.0449).

Basal cells and dust-laden macrophages. Very few collections of dust-laden macrophages were identified, and measurements were limited to generations 4–16 (Fig. 8). The distances from these macrophages to the nuclei of typical basal cells vary from 4.11–9.03 μm; for atypical basal cells, the range is 3.4–4.0 μm.

Thickness of epithelium and anatomical location. Comparisons between different lobes of the lung show that the thickness of epithelium declines with each subsequent generation, and the thicknesses of epithelium and basement membrane are similar for bronchi of the same generation regardless of the lobe examined.

Metaplasia and hyperplasia. These changes are patchy in nature, and in many of the cases examined, including the nonsmokers, metaplasia and hyperplasia are unusual findings. The figures shown in Table 6 are from smokers only. There is no significant variation between the measurements recorded for different generations. The distance between the surface of metaplastic epithelium and the basement membrane varies between 27.56 μm and 49.83 μm; the hyperplastic epithelium shows a range of 37.08 μm to 47.49 μm.

Artefacts of tissue preparation

Fixation in 10% buffered formalin caused shrinkage (3.85% ± 0.52%) but was almost entirely compensated by expansion (3.10 ± 1.77%) during preparation of methacrylate sections. The final preparation artefact was 0.75%.

Fig. 4a. Bronchial epithelium showing typical (1) and atypical (2) basal cells. Toluidine blue–basic fuchsin.

DISCUSSION

The high incidence of pulmonary cancer in U miners is thought to be related to U decay with the production of Rn daughters that attach to molecules of water or to particles of dust to form "cluster ions." The depth of tissue penetration by α particles is short and it is important to know if the nuclei of epithelial cells and, in particular, the nuclei of basal cells are within range of these particles.

In an earlier retrospective study, Gastineau et al. (1972) measured the bronchial epithelium in paraffin sections of specimens previously submitted for pathologic diagnosis. The smoking history, age, and sex of the patients are unknown. Artefacts such as shrinkage were assessed by measuring the diameters of erythrocytes in the sections and comparing these measurements with the established "physiologic" diameter of erythrocytes.

The present study is based on measurements made on freshly obtained pulmonary tissue removed by pneumonectomy or lobectomy from 29 patients. Particular attention was given to the methods of preparation and to the determination of a factor for the correction of artefacts arising during preparation. The 3.85% shrinkage caused by fixation is almost completely compensated by subsequent expansion during preparation of the methacrylate

Fig. 3b. Bronchial epithelium. Toluidine blue–basic fuchsin.

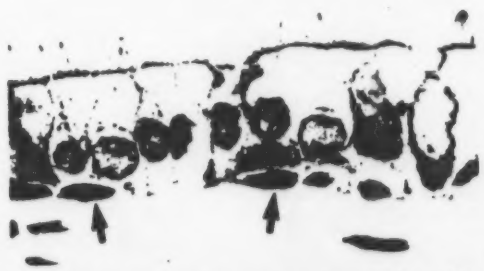

Fig. 4b. Atypical basal cells (arrows) arranged circumferentially in bronchial epithelium. Toluidine blue–basic fuchsin.

Table 3. Epithelial thickness (μm): surface of cell to basement membrane (smokers and nonsmokers).

Smoking history/pack years	<25	≥25	≥50	≥100	Nonsmokers	p value
Cell type						
Bronchial generation 4						
Ciliated	33.36 ± 15.30	25.19 ± 4.62	22.48 ± 2.47	28.93[a]	25.51 ± 2.46	0.6601
Ciliated (+ cilia)	39.27 ± 15.37	31.98 ± 4.80	28.32 ± 2.64	34.90[a]	31.23 ± 2.45	0.6734
Non-ciliated	22.76 ± 0.79	23.92 ± 3.47	26.16 ± 3.85	25.11[a]	27.60 ± 1.51	0.8372
Goblet	40.92 ± 7.67	26.31 ± 3.93	28.83 ± 0.89		26.16 ± 2.87	0.0843
Bronchial generation 5–7						
Ciliated	30.41 ± 6.37	26.46 ± 2.74	28.68 ± 2.96	28.56 ± 1.54	20.67 ± 1.01	0.6323
Ciliated (+ cilia)	35.97 ± 10.87	32.29 ± 2.70	34.49 ± 2.97	34.64 ± 1.80	26.32 ± 1.02	0.6225
Non-ciliated	14.52[a]	20.10 ± 2.43	24.82 ± 2.93	22.21 ± 5.93	16.44 ± 0.91	0.3748
Goblet	39.19 ± 8.95	29.85 ± 3.78	31.68 ± 2.86	33.45 ± 2.17	23.56 ± 1.74	0.4176

[a] Absence of standard error due to insufficient number of cases. Numbers represent mean ± standard error. *p* values are for comparisons of all columns.

sections. The final correction factor for shrinkage is 0.75%. Although it is not possible to compare this factor to that used by Gastineau et al. (1972), it is generally held that a considerable amount of shrinkage occurs during the preparation of paraffin sections. Furthermore, the relatively poor resolution obtained by light microscopy using routine paraffin sections limits the precision of measurements.

Selection of the methacrylate method and its implementation under carefully controlled conditions appear to reduce artefacts to a minimum and enhance the precision of measurements because of the improved resolution achieved with 1.5 μm sections. We emphasize, however, that the correction factor established in this investigation applies only to the precise method used; it is not transferable to specimens of lung prepared in a different manner, and it should not be used for tissues other than the lung.

All of the parameters of epithelial thickness (Fig. 1) were for typical bronchial epithelium from 26 smokers and 3 nonsmokers. The disparity between the number of smoking and nonsmoking patients in this study is a reflection of the scarcity of surgically resected lung from nonsmoking patients; no additional cases were available. The 26 patients with a history of smoking were selected from a much larger pool; numerous lungs were excluded from the study because of the extent of lesions. No significant differences between the two groups were found and for subsequent analyses the 29 cases were treated as a homogeneous group.

The results are similar to those of Gastineau et al. (1972) in that the thickness of the epithelium decreases progressively with successive generations. However, where direct comparisons are possible, our measurements indicate the bronchial epithelium to be thinner than was reported by Gastineau et al. (1972) (Table 7).

Of more importance than the overall thickness are the measurements of the distances from the luminal surfaces of the cells to the underlying nuclei. The figures given by Gastineau et al. (1972) relate specifically to the basal cells. They estimated that over two-thirds of basal cells in the lobar and segmental bronchi, that is, generations 2–16 (Weibel 1963), were within range of 7.69-MeV ^{214}Po α particles and about one-fifth were within range of 6.0-MeV ^{218}Po particles.

Studies in animals indicate that, in addition to basal cells, other cells including nonciliated columnar cells, with or without secretory granules, are capable of dividing (Bindreiter et al. 1968; Lane and Gordon 1974; Becci et al. 1978; Boren and Paradise 1978; Donnelly et al. 1982; Evans et al. 1986), and secretory cells may, on occasion, be the progenitors of other bronchial cells (Keenan et al. 1982a, 1982b; McDowell et al. 1984, 1985). In the present study, measurements include the distances from the luminal surface to the nuclei of all cell types.

Combining the figures for smokers and nonsmokers.

Table 4. Ciliary height and epithelial thickness (μm): surface of cell to basement membrane (composite data, smokers, and nonsmokers).[a]

Bronchial generation Bronchial diameter (mm)	1 >9.01	2 7.01–9	3 5.51–7	4 4.51–5.50	5–7 2.01–4.50	7–16 0.26–2	p value
Cell type							
Ciliary height	6.52 ± 0.21	6.40 ± 0.41	6.29 ± 0.21	6.02 ± 0.18	5.84 ± 0.13	5.58 ± 0.12	0.0020
Ciliated	31.17 ± 2.23	31.98 ± 4.87	29.02 ± 3.03	25.32 ± 2.13	27.35 ± 1.63	20.94 ± 1.37	0.0051
Non-ciliated	29.57 ± 4.77	32.91 ± 2.90	23.65 ± 3.07	24.99 ± 1.24	21.51 ± 1.67	17.76 ± 1.19	0.0038
Goblet	31.65 ± 2.67	30.23 ± 6.23	32.24 ± 3.21	30.76 ± 2.30	31.28 ± 1.92	26.96 ± 2.77	0.7787

[a] Numbers represent means ± standard error. *p* values are for comparing all columns.

Table 5. Epithelial thickness (μm): surface of cell to nucleus (composite data, smokers, and nonsmokers).[a]

Bronchial generation Bronchial diameter (mm)	1 >9.01	2 7.01–9	3 5.51–7	4 4.51–5.50	5–7 2.01–4.50	7–16 0.26–2	*p* value
Cell type							
Ciliated	12.86 ± 1.42	10.96 ± 1.79	9.42 ± 0.99	8.61 ± 0.75	9.14 ± 0.60	6.53 ± 0.52	0.0010
Non-ciliated	10.08 ± 2.49	13.05 ± 1.67	9.10 ± 1.59	9.10 ± 1.09	7.32 ± 0.53	6.41 ± 0.59	0.0167
Goblet	19.83 ± 1.77	18.42 ± 3.05	19.42 ± 1.39	19.37 ± 1.58	20.32 ± 1.30	18.11 ± 2.07	0.9430
Basal (typical)	26.65 ± 2.36	25.83 ± 3.96	24.08 ± 2.22	22.02 ± 1.29	24.59 ± 1.76	17.46 ± 0.93	0.0033
Basal (atypical)	23.34 ± 2.40	21.33 ± 5.07	17.19 ± 1.36	20.11 ± 1.84	18.15 ± 1.08	15.98 ± 1.19	0.0686

[a] Numbers represent means ± standard error. *p* values are for comparing all columns.

Table 6. Epithelial thickness (μm): hyperplasia and metaplasia.

Bronchial generation	1	2	3	4	5–7	7–16
Hyperplasia	43.95 ± 3.61	47.49 ± 1.66	45.92 ± 5.84	43.45 ± 8.97	43.02 ± 2.59	37.08 ± 4.39
Metaplasia	35.01 ± 6.56	24.14[a]	27.56 ± 4.36	35.47 ± 6.92	29.97 ± 3.37	49.83 ± 31.00

[a] Absence of standard error due to insufficient number of cases. Numbers represent means ± standard error.

we find that, with the exception of goblet cells and nonciliated cells, the measurements in generations 7–16 are significantly less than those in generation 1, the largest bronchi (Fig. 5). The progressive decrease in epithelial thickness through descending bronchial generations is shown in Table 4. The nuclei of cells in generation 1 are farther from the surface than any other cells in the bronchi; for basal cells, this distance is less than 27 μm; for goblet cells it is less than 20 μm, and the nuclei of ciliated and nonciliated cells are not more than 13 μm from the luminal surface of these cells. In generations 7–16, the nuclei of all cells are within 7–17 μm of the surface.

Nuclear size may be of some importance in computing biologically effective radiation dosage. The nuclei of the specific cell types are of different size; and no significant differences of nuclear size are found in generations 1–16 of the bronchial tree.

The figures given in the tables and graphs depict the measurements from the luminal surface to the nuclei. They do not include the mucous layer or the cilia. The thickness of the mucous layer is unknown although it probably varies in smokers and nonsmokers; the distribution and relative solubility of Rn daughters in mucus remain ill-defined. Since it was not possible to measure the mucous layer, it has been estimated to be 5 μm, and an average of 6 μm has been allocated for the cilia. The small shrinkage factor (0.75%) has been ignored.

The composite figures derived by combining these estimates with actual measurements are presented in a form that may be useful in assessing the total distances separating epithelial nuclei from radioactive particles impinging on the surface of the mucus lining the bronchi (Table 8). All epithelial nuclei of the bronchial tree lie between 17 and 38 μm of the mucous layer. This means

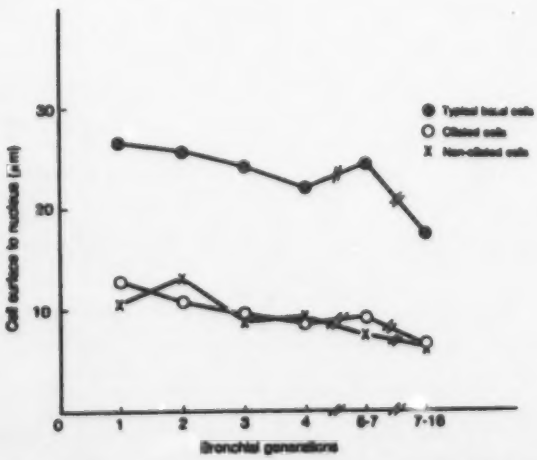

Fig. 5. Measurements from cell surfaces to nuclei by bronchial generation (μm). Composite data, smokers and nonsmokers.

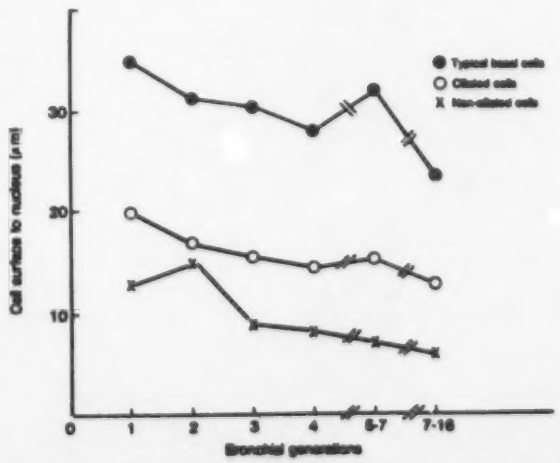

Fig. 6. Measurements from cell surfaces to nuclei by bronchial generation (μm) for smokers.

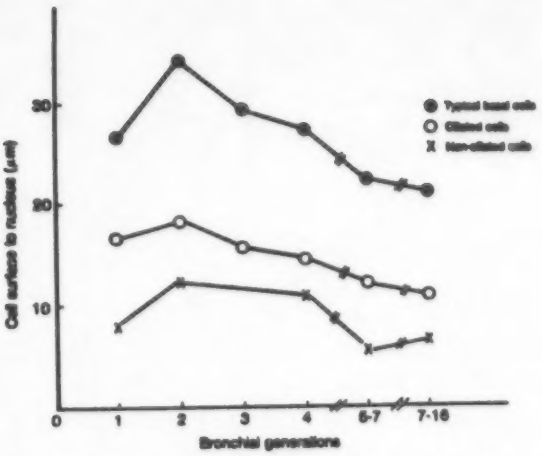

Fig. 7. Measurements from cell surfaces to nuclei by bronchial generation (μm) for nonsmokers.

that all of these nuclei are within the 47 μm range of 6.0-MeV ^{218}Po particles. A 7.69-MeV ^{214}Po particle could affect a nucleus up to 70.8 μm distant (Lea 1955). Similarly, all nuclei of smokers (Fig. 6) and nonsmokers (Fig. 7) are within range.

Gastineau et al. (1972) calculated that more than two-thirds of the basal cells in lobar and segmental bronchi (generations 2–16) are within the range of the ^{214}Po α particles and about one-fifth are within the range of the ^{218}Po α particles; basal cells in the thicker epithelium of the main stem bronchi were outside this range. The results of the present study indicate that all epithelial nuclei, including those of the basal nuclei, in all bronchial generations are within the range of an α particle source on the mucous surface at all levels of the bronchial tree.

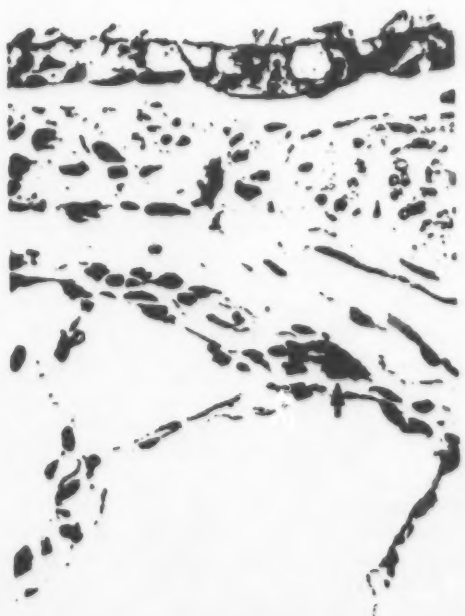

Fig. 8. Dust-laden macrophage (arrow) in the interstitium. Toluidine blue–basic fuchsin.

Table 7. Epithelial thickness (μm). Data of Gastineau et al. (1972) compared with present study.

Bronchus	Mean thickness (μm)		Difference (%)
	Gastineau et al. (1972)	Baldwin et al.	
Main stem (Generation 1*)	80	40	−50
Lobar (Generation 2*)	50	39	−22
Segmental (Generation 3*)	50	36	−28
Subsegmental (Generations 4–16*)	50	33	−34

* Weibel (1963).

As the total number of airways increases with successive generations, the small bronchioles lie closer to each other. This introduces the possibility that nuclei in one bronchiole may fall within the range of radioactive particles in an adjacent airway. Calculations derived from the work of Weibel (1963) and from our own measurements reveal that the bronchial tree occupies such a small proportion of the total volume of the lung that the distance from the mucociliary surface of one conducting airway to the nuclei of another exceeds the range of α particles. The nuclei of interstitial cells may, of course, be at risk.

Most of the lungs examined showed scattered small areas of epithelial hyperplasia and squamous metaplasia. These changes are of interest because they are found more frequently in the lungs of smokers (Auerbach et al. 1956, 1957; Sanderud 1958). This raises the question of the relationship, if any, between metaplasia and neoplasia. Two factors may be considered: the lack of a protective mucociliary layer and thickness of the altered epithelium. The absence of ciliary movement inhibits clearance, allowing inhaled particles to remain on the surface. This may increase the duration of exposure to irradiation and, possibly, increase the chances of epithelial penetration. A thin epithelium would magnify these hazards.

Table 8. Calculated figures of mean distances of nuclei from mucociliary surface (μm) (see text).

Cell type	Generation 1	Generations 7–16
Basal cells (typical)	38	28
Basal cells (atypical)	34	27
Goblet cells	31	29
Ciliated cells	24	18
Non-ciliated cells	21	17

Table 6 gives the mean thickness of the areas of metaplasia in all bronchial generations. Given the absence of cilia, all nuclei in the metaplastic epithelium are within the range of radioactive particles on the surface. Furthermore, the range of measurements is large, with some metaplastic areas being very thin indeed.

The significance of the long-term pulmonary retention of radioactive dust in perivascular and peribronchiolar regions is unknown. None of the lungs examined in this study showed heavy accumulations of dust, and we recorded only a few measurements of the distances between dust-laden macrophages and the nuclei of basal epithelial cells. The range of figures, 3.43–9.03 μm, suggests that aggregates of radioactive dust in peribronchiolar sites could, depending upon their half-lives and energies, affect the basal cells of the bronchi.

Acknowledgment—This research was supported by the Atomic Energy Control Board of Canada.

REFERENCES

Auerbach, O.; Gere, J. B.; Forman, J. B.; Petrick, T. G.; Smolin, H. J.; Muehsam, G. E.; Kassouny, D. Y.; Stout, A. P. Changes in the bronchial epithelium in relation to smoking and cancer of the lung. N. Engl. J. Med. 256:97–104; 1957.

Auerbach, O.; Petrick, T. G.; Stout, A. P.; Statsinger, A. L.; Muehsam, G. E.; Forman, J. B.; Gere, J. P. The anatomical approach to the study of smoking and bronchogenic carcinoma. Cancer 9:76–83; 1956.

Becci, P. J.; McDowell, E. M.; Trump, B. F. The respiratory epithelium. II. Hamster trachea, bronchus and bronchioles. J. Natl. Cancer Inst. 61:551–561; 1978.

Bindreiter, M.; Shuppler, J.; Stockinger, L. Zellproliferation und Differenzierung im Trachealepithel der Ratte. Exp. Cell Res. 50:377–382; 1968.

Boren, H. G.; Paradise, L. J. Cytokinetics of the lung. In: Harris, C. C., ed. Pathogenesis and therapy of lung cancer. New York: Marcel Dekker; 1978:369–418.

Chamberlain, A. C.; Dyson, E. D. The doses to the trachea and bronchi from the decay products of radon and thoron. Br. J. Radiol. 29:317–327; 1956.

Committee on the Biological Effects of Ionizing Radiation (BEIR III). Health risks of radon and other internally deposited alpha-emitters. Washington, D.C.: National Academy Press; 1980.

Committee on the Biological Effects of Ionizing Radiation (BEIR IV). Health risks of radon and other internally deposited alpha-emitters. Washington, D.C.: National Academy Press; 1988.

Davies, C. N. Aerosol sampling related to inhalation. In: Assessment of airborne radioactivity. Symposium on instruments and techniques for the assessment of airborne radioactivity in nuclear operations. Vienna: International Atomic Energy Agency; 1967:3–22.

Davies, C. N. Deposition of inhaled particles in man. Chem. Ind. (London) 11:441–444; 1974.

Donnelly, G. M.; Haack, D. G.; Heird, C. S. Tracheal epithelium: Cell kinetics and differentiation in normal rat tissue. Cell Tissue Kinet. 15:119–130; 1982.

Evans, M. J.; Shami, S. G.; Cabral-Anderson, L. J.; Dekker, N. P. Role of non-ciliated cells in renewal of the bronchial epithelium of rats exposed to NO_2. Am. J. Pathol. 123:126–133; 1986.

Gastineau, R. M.; Walsh, P. J.; Underwood, N. Thickness of bronchial epithelium with relation to exposure to radon. Health Phys. 23:857–860; 1972.

Horacek, J.; Placek, V.; Sevc, J. Histological types of bronchogenic cancer in relation to different conditions of radiation exposure. Cancer 40:832–835; 1977.

International Committee on Radiological Protection. Lung cancer risk from indoor exposures to radon daughters. Oxford: Pergamon Press; Ann. ICRP 7:1; 1987.

Keenan, K. P.; Combs, J. W.; McDowell, E. M. Regeneration of hamster tracheal epithelium after mechanical injury. I. Focal lesions: Quantitative morphological study of cell proliferation. Virchows Arch. (Cell Pathol.) 41:193–214; 1982a.

Keenan, K. P.; Combs, J. W.; McDowell, E. M. Regeneration of hamster tracheal epithelium after mechanical injury. II. Multifocal lesions: Stathmokinetic and autoradiographic studies of cell proliferation. Virchows Arch. (Cell Pathol.) 41:215–229; 1982b.

Lane, B. P.; Gordon, R. Regeneration of rat tracheal epithelium after mechanical injury. I. The relationship between mitotic activity and cellular differentiation. Proc. Soc. Exp. Biol. Med. 145:1139–1144; 1974.

Lea, D. E. A. Action of radiation on living cells. 2nd ed. Cambridge, MA: Cambridge University Press; 1955.

McDowell, E. M.; Keenan, K. P.; Huang, M. Restoration of mucociliary tracheal epithelium following deprivation of vitamin A. Virchows Arch. (Cell Pathol.) 45:221–240; 1984.

McDowell, E. M.; Newkirk, C.; Coleman, B. Development of hamster tracheal epithelium. II. Cell proliferation in the fetus. Anat. Rec. 213:448–456; 1985.

Saccamano, G.; Archer, V. E.; Auerbach, O.; Kuschner, M.; Saunders, R. P.; Klein, M. G. Histological types of lung cancer among uranium miners. Cancer 27:515–523; 1971.

Sanderud, K. Squamous metaplasia of the respiratory tract epithelium. Acta. Pathol. Microbiol. Scand. 43:47–61; 1958.

Sevc, J.; Kunz, E.; Tomasek, L.; Placek, V.; Horacek, J. Cancer in man after exposure to Rn daughters. Health Phys. 54:27–46; 1988.

Webster, I. Bronchogenic carcinoma in South African gold miners. In: Shapiro, H. A., ed. Pneumoconeosis, Proceedings of the international conference, Johannesburg. Cape Town: Oxford University Press; 1969:572–574.

Weibel, E. R. Morphometry of the human lung. New York: Academic Press; 1963.

Weiss, D. L.; Tweedale, D. N. Inflation fixation of lungs: Use of a simple, inexpensive apparatus. Am. Rev. Resp. Dis. 94: 629–631; 1966.